Identifying Genetic Basis and Molecular Mechanisms in Different Types of von Willebrand Disease (VWD)

Dissertation
zur
Erlangung des Doktorgrades (Dr. rer. nat.)
der
Mathematisch-Naturwissenschaftlichen Fakultät
der
Rheinischen Friedrich-Wilhelms-Universität Bonn

vorgelegt von

Hamideh Yadegari

aus

Esfahan, Iran

Bonn, März 2013

Angefertigt mit Genehmigung der
Mathematisch Naturwissenschaftlichen Fakultät der
Rheinischen Friedrich-Wilhems-Universität Bonn

1. Gutachter: Prof. Dr. Johannes Oldenburg

2. Gutachter: Prof. Dr. Evi Kostenis

Tag der Promotion: 17.07.2013
Erscheinungsjahr: 2013

Dedicated to my parents

For their endless love, support and encouragement

Abbreviations

aa	amino-acid
ADAMTS13	a disintegrin-like and metalloprotease domain with thrombospondin type-1 motif, number 13
aPTT	Activated partial thromboplastine time
ASA	Average surface accessible area
Bp	Base pair
BS	Bleeding score
BSS	Bleeding severity score
cAMP	Cyclic adenosine monophosphate
cDNA	Complementary Deoxynucleic acid
CK	Cysteine knot
C-terminal	Carboxy-terminal
C8	Cysteine 8
Da	Dalton
db	Database
DDAVP	Vasopressin analogue, 1-desamino-8-D-arginine-vasopressin
dl	Deciliter
DMEM	Dulbecco’s Modified Eagle’s Medium
DNA	Deoxynucleic acid
DSS	Donor splice site
EDTA	Ethylenediamintetraacetic acid
ELISA	Enzyme-linked immunosorbent assay
ER	Endoplasmic reticulum
FBS	Fetal bovine serum
FVIII	Factor VIII
FVIII:C	Factor VIII activity
F8	Factor VIII gene
GPIb	Platelet glycoprotein Ib
GPIIb–IIIa	Glycoprotein IIb–IIIa
HEK 293	Human embryonic kidney 293 cells

HMW	High-molecular weight
HMWM	High-molecular weight multimers
Hr	Hour
IP	Index patient
ISTH SSC	International Society on Thrombosis and Haemostasis Scientific and Standardisation Committee
IU	International unit
kb	Kilo base pair
kDa	Kilo Dalton
MD	Molecular dynamic
mg	Miligram
min	Minute
ml	Milliliter
MLPA	Multiplex ligation-dependent probe amplification
mRNA	Messenger RNA
µg	Microgram
µm	Micrometer
N	Normandy
ns	Nanosecond
nt	Nucleotide
PBS	Phosphate Buffered Saline
PCR	Polymerase chain reaction
PDI	Protein disulphide isomerase
PFA-100	Platelet function analyzer 100
PolyPhen	Polymorphism Phenotyping
RER	Rough endoplasmic reticulum
RGD	Arg-Gly-Asp
RIPA	Ristocetin induced platelet aggregation
RNA	Ribonucleic acid
ROG	Radius of gyration
rVWF	Recombinant von Willebrand factor
SDS	Sodium dodecyl sulfate
SIFT	Sorting Intolerant From Tolerant

TGN	Trans-Golgi network
TIL	Trypsin-inhibitor-like
UL-VWF	Ultra large von Willebrand factor
VWC -domain	von Willebrand C-domain
VWD	von Willebrand disease
VWD-domain	von Willebrand D-domain
VWF	von Willebrand factor
VWF	VWF gene
VWF:Ag	von Willebrand factor antigen
VWF:CB	von Willebrand factor: collagen binding
VWF:FVIIIB	VWF: FVIII binding
VWF:GPIbB	von Willebrand factor: GPIb binding
VWF:RCo	von Willebrand factor: ristocetin cofactor
WPB	Weibel-Palade body
WT	Wild type

Summary

Von Willebrand disease (VWD) is the most common inherited bleeding disorder. It is caused by quantitative or qualitative defects of the von Willebrand factor (VWF) which has crucial roles in hemostasis. VWD is classified into three primary categories. Types 1 and 3 represent partial and total quantitative deficiency of VWF, respectively. Type 2 is due to qualitative defects of VWF, and is divided into four secondary categories 2A, 2B, 2M and 2N. In this study we explored genotype and phenotype characteristics of a cohort of VWD patients with the aim of dissecting the distribution of mutations in different types of VWD. Mutation analysis of 114 patients diagnosed to have VWD was performed by direct sequencing of the VWF gene (*VWF)*. Large deletions were investigated by multiplex ligation-dependent probe amplification (MLPA) analysis. The results showed a mutation detection rate of 68%, 94% and 94% for VWD type 1, 2 and 3, respectively. In total, 68 different putative mutations were detected. Twenty six of these mutations were novel. In type 1 and type 2 VWD, the majority of identified mutations (74% vs 88.1%) were missense substitutions while mutations in type 3 VWD mostly caused null alleles (82%). In addition, the impact of five detected novel cysteine missense mutations residing in D4-CK domains was characterized on conformation and biosynthesis of VWF. Transient expression of human cell lines with wild-type or five mutant VWF constructs was done. Quantitative and qualitative assessment of mutated recombinant VWF was performed. Storage of VWF in pseudo-Weible-Palade bodies (WPBs) was studied with confocal microscopy. Moreovere, structural impact of the mutations was analyzed by homology modeling. Homozygous expressions showed that these mutations caused defects in multimerization, elongation of pseudo-WPBs and consequently secretion of VWF. Co-expressions of wild-type VWF and 3 of the mutants demonstrated defect in multimer assembly, suggesting a new pathologic mechanism for dominant type 2A VWD due to mutations in D4 and B domains. Structural analysis revealed that mutations either disrupt intra-domain disulfide bonds or might affect an inter-domain disulfide bond.

In conclusion, our study extends the mutational spectrum of *VWF*, and improves the knowledge of the genetic basis of different types of VWD. The gene expression studies highlight the importance of cysteine residues within the C-terminal of VWF on the structural conformation of the protein and consequently multimerization, storage, and secretion of VWF.

Table of Contents

Chapter 1

General introduction and outline

1.1 VWF

Von Willebrand factor (VWF) is a large multimeric plasma glycoprotein that first was identified by Zimmermann in 1971.[1, 2] The VWF plays a crucial role in hemostasis. It mediates platelet adhesion in primary hemostasis. In addition, VWF carries factor VIII (FVIII) in the circulation, protecting it from rapid proteolytic degradation and delivering it to sites of vascular damage for secondary hemostasis.[1, 3] Normal circulating VWF is composed of a series of heterogeneous multimers ranging in size from about 500 kDa to over 20000 kDa.[4] The mean plasma level of VWF is 100 IU dL^{-1} but the population distribution is between 50 IU dL^{-1} and 200 IU dL^{-1}.[5] Many factors such as ABO blood group, gender, age, hormonal regulation, and inflammatory states have been described to have an impact on VWF levels.[6]

Deficient or defective VWF results in von Willebrand disease (VWD), a common inherited bleeding disorder.[7]

1.1.1 VWF gene

The VWF gene (*VWF*) is located on the short arm of chromosome 12 (12p 13.2). It spans approximately 178 kb of genomic DNA, and is transcribed into an 8.8 kb mRNA. The VWF gene comprises 52 exons, most exons are ranging from 40-342 bp, but exon 28 is exceptionally larger (1.4 kb in size).[1, 8] A non-coding partial VWF pseudogene has been identified on chromosome 22 (22q11.22 to 22q11.23). The pseudogene is 97% similar in sequence to the coding gene, corresponding to exons 23 to 34 of *VWF*. Gene conversion events between *VWF* and VWF pseudogene have been demonstrated.[9, 10] *VWF* is highly polymorphic with about 200 reported polymorphic variations in *VWF* recorded in the International Society on Thrombosis and Haemostasis Scientific and Standardisation Committee on VWD database (ISTH SSC-VWD db http://vwf.group.shef.ac.uk/index.html accessed January 2013). This highly polymorphic nature of *VWF,* along with its large size and the presence of a partial pseudogene make genetic analysis of *VWF* challenging.[10, 11]

1.1.2 VWF protein structure and domain organization

The VWF monomer is comprised of 2813 amino acids (aa). The VWF protein is remarkably rich in cysteines, which comprise 234 of the 2813 (8,3%) residues in prepro VWF.[3, 12] The VWF protein is extensively glycosylated, oligosaccharide side chains make up approximately 20% of the mass of VWF, and are believed to affect its structural and functional integrity .[13]

The prepro VWF precursor is composed of five types of domains that are constructed as repeats in the following order: D1-D2-D'-D3-A1-A2-A3-D4-B1-B2-B3-C1-C2-CK (Figure 1.1 A).[14] The D1 and D2 domains comprise the propeptide and are cleaved during proteolytic processing to generate the mature VWF. The remaining domains in the mature VWF carry out specific functions. [2, 15]

The domains may be characterized as structural or functional, depending on their role in VWF structure or its interaction with other factors. Structural domains are involved in the post-translational processing of VWF, for example the cysteine knot (CK) domain is required for dimerization of VWF monomers and the D1, D2 and D3 domains for proper multimerization of VWF dimers.[16] All 'D' domains (except D4) contain a CGLC consensus sequence that is highly homologous to the active site of proteins harbouring protein disulphide isomerase (PDI) activity.[16, 17, 18] PDI is the enzyme that catalyses thiol-disulphide interchange reactions in protein substrates, leading to disulphide formation and folding of the protein.[17] In this respect, ability of the D1, D2 and D3 domains to promote interchain disulphide bonding and multimerization can be ascribed to the intrinsic PDI activity of these domains.[17, 18]

Functional domains include those that contain cleavage sites for proteolysis (domain A2) and binding sites for collagen (domains A1 and A3), platelets (domain A1 for platelet glycoprotein Ib (GPIb) receptors), and FVIII (domains D3 and D') (Figure 1.1A).[16, 18] Moreover, the C1 domain contains the RGD sequence (Arg-Gly-Asp) recognized by platelet integrin GPIIb/IIIa receptors. Another RGD sequence is present in the propeptide, but no role in integrin binding has been observed. [3, 17] The carboxy-terminal domains, namely D4-B1-3-C1-2, are cysteine-rich, which may suggest structural importance.[16]

Recently, Zhou *et al*. have re-evaluated the VWF domain structure, using the updated information on the structure of these homologous domains in combination with electron microscopy techniques.[14, 19] The previous B and C regions of VWF are re-annotated as 6 tandem von Willebrand C (VWC) and VWC-like domains.[19] Moreover, the VWF D domains are annotated as containing von Willebrand D (VWD-domain), cysteine 8 (C8), trypsin-inhibitor-like (TIL), E or fibronectin type 1-like domains and a unique D4N sequence in D4 (Figure 1.1B). However, the original domain designations still predominate in the VWF literature.

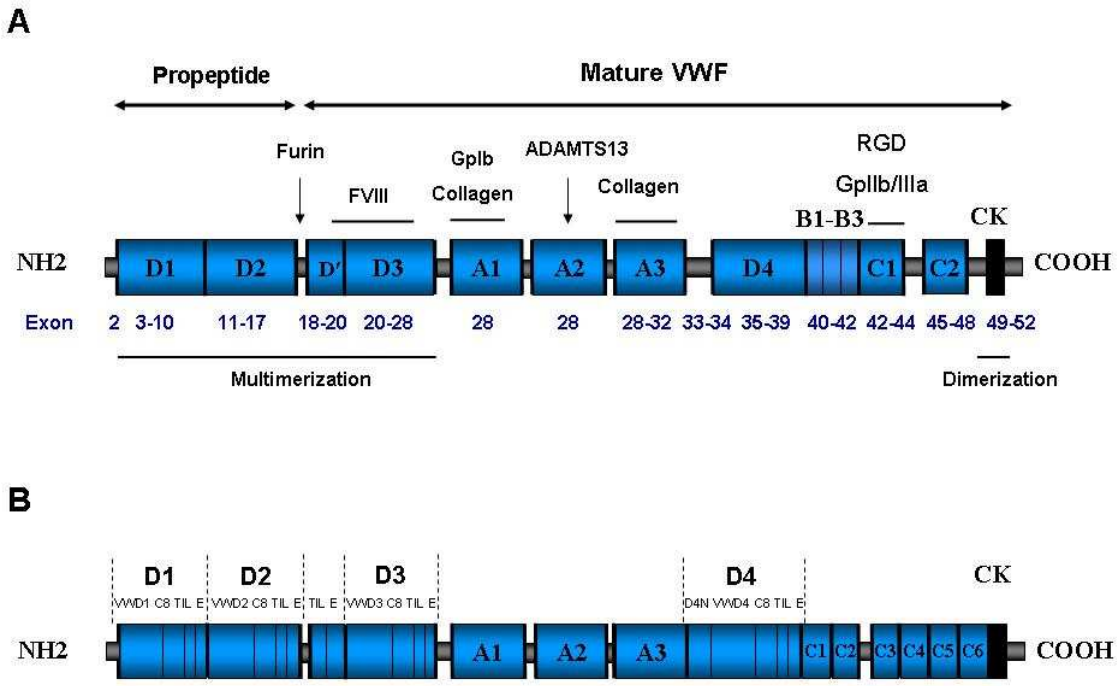

Figure 1.1. Structural and functional domains of von Willebrand factor (VWF). Part A illustrates the original domain assignment of VWF along with binding and cleavage sites, as well as dimerization and multimerization regions. Exons encoding each domain are shown (adapted from Goodeve AC)[1]. **Part B** illustrates the updated domain annotation of VWF (adapted from Zhou YF *et al.*)[19].

1.1.3 VWF biosynthesis

VWF is produced exclusively by endothelial cells present in different tissues and by the platelet precursor, megakaryocytes.[2, 17] Platelet VWF is stored within cells and has not been shown to contribute significantly to plasma VWF.[13]
The VWF primary translation product is a 2813-aa pre-pro-polypeptide (350 kDa) which encompasses a 22-aa classic signal sequence, a 741-aa propeptide and a 2050-aa mature VWF protein.[17, 20] Posttranslational processing of VWF includes dimerization, glycosylation, sulfation, propeptide cleavage, and multimerization, followed by storage or secretion (Figure 1.2).[3]

Dimerization and multimer assembly

After the cleavage of the signal peptide and translocation into the endoplasmic reticulum (ER), pro-VWF subunits dimerize in a 'tail-to tail' manner through disulfide bonds that form between the C-terminal residues (Figure 1.2).[2, 3] The dimerization function requires only sequences within the last 150 residues. The cysteins within the last 150 aa residues of the VWF subunit form intersubunit or intrasubunit disulfide bonds. The carboxyl-terminal 90 residues comprise the "CK" domain that is homologous to the "Cysteine knot" superfamily of proteins. The family members share a tendency to dimerize, often through disulfide bonds.[15, 21]
The pro-VWF dimers are subsequently transported to the Golgi complex, where multimerization and the proteolytic removal of the large VWF peptide take place (Figure 1.2).[2] In the Golgi apparatus and post-Golgi compartments, dimers undergo multimerization to form tetramers, hexamers and so on, generating high-molecular weight (HMW) multimers containing up to 100 monomers that may exceed 20 million Da in size.[18] Multimerization occurs through additional head-to-head disulfide bonds near the amino-termini of the subunits.[3] The VWF multimer assembly appears to involve an unique oxidoreductase mechanism that is activated by the low pH of the Golgi apparatus.[15] The key to multimer assembly is the N-terminal D1-D2-D'-D3 region of proVWF. The reaction appears to proceed through a transient, disulfide-linked intermediate between

the propeptide and the D3 region of VWF that forms in the ER and resolves in the Golgi to yield disulfide-linked VWF multimers.[22]

The polymerization process is accompanied by proteolytic cleavage (probably by furin) of the propeptide in the trans-Golgi network, yielding mature VWF multimers and propeptide dimers. The propeptide cleavage occurs after the argenine residue at position 763. After cleavage, VWF and the VWF propeptide remain non-covalently associated within the cell.[15, 17]

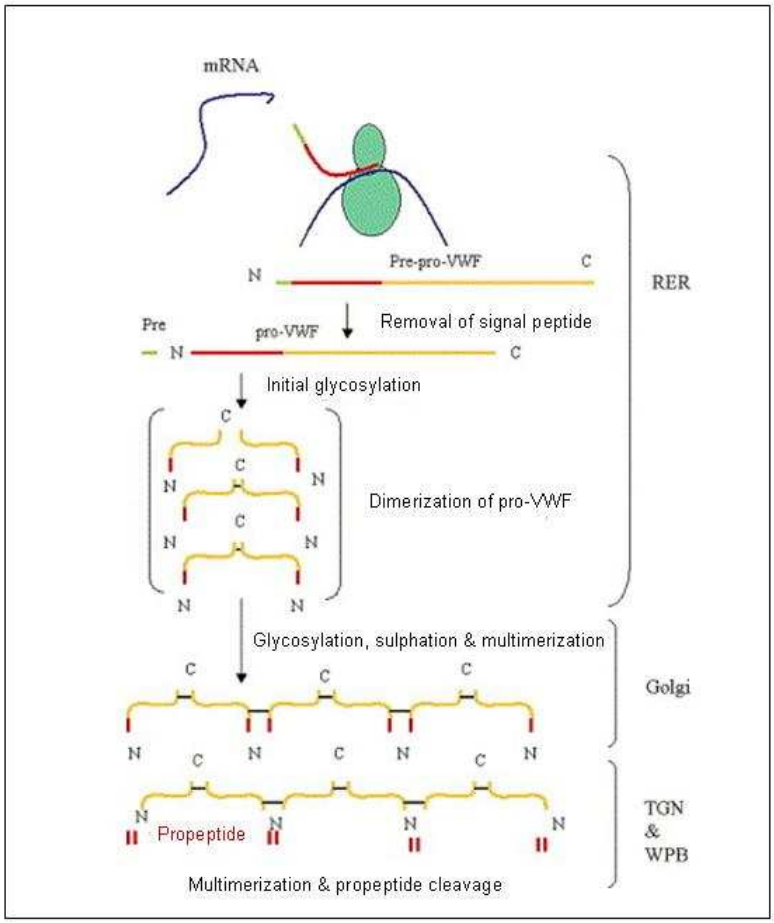

Figure 1.2. Biosynthesis of VWF (adapted from Millar CM et al.).[13]
After the cleavage of the signal peptide and translocation into the rough endoplasmic reticulum (RER), initial glycosylation and dimerization of pro-VWF takes place. The pro-VWF dimers are subsequently transported to the Golgi complex, where they undergo post-translational glycosylation, sulphation and multimerization. Finally, the propeptide is cleaved in the trans-Golgi network (TGN) and fully functional VWF multimers are stored in Weibel-Palade bodies (WPB).

Glycosylation, sulfation

The mature subunit is extensively glycosylated with 12 N-linked and 10 O-linked oligosaccharides, and the propeptide has three more potential N-glycosylation sites.[12] The N-linked carbohydrates are added in high-mannose form in the ER and are further processed to complex forms in the Golgi apparatus. O-glycosylation and sulfation of some N-linked oligosaccharides also occur in Golgi compartments.[23, 24] The N-linked oligosaccharides of VWF are unusual compared to those of other plasma glycoproteins because they contain ABO blood group oligisacharides.[12] The antigens of the ABO blood group system (A, B, and H determinants, respectively) consist of complex carbohydrate molecules. It is demonstrated that ABH structures are carried on the N-linked oligosaccharide chains of VWF according to the blood type of the individual.[23, 25]

Intracellular storage

VWF produced by endothelial cells is either secreted constitutively or stored in Weibel-Palade bodies (WPBs), while VWF produced by megakaryocytes that are later converted into platelets, is stored in α-granules.[12]

WPBs are rod-shaped, membrane enclosed organelles, approximately 0.2 μm wide and up to 5 μm long.[15, 17] They consist of densely packed tubular arrays of VWF which are composed of VWF multimers and propeptide. Tubulation allows a 100-fold compaction of VWF, without which intracellular storage of VWF would be impossible. In addition, the tubular storage of VWF multimers is critical for the orderly secretion of long VWF strings without tangling.[12, 26]

WPBs initially form at the TGN and subsequently undergo maturation, before accumulating within the cytoplasm of endothelial cells. The VWF multimers and propeptide condense into tubules and are incorporated into nascent vesicles that protrude from the TGN. After budding from the TGN, immature WPBs remain in a perinuclear location, where they acquire additional membrane proteins and then disperse throughout the cytoplasm.[20, 27]

The VWF is a prerequisite for the existence of WPBs.[28] It has been proposed that the targeting of VWF to the WPBs occurs as a consequence of selective

aggregation, by means of multimerization of this protein in the trans-Golgi network.[27, 29] The N-terminal D1-D2-D'-D3 domains and the acidic pH of the trans-Golgi are required to target and package VWF into WPBs. Thus, multimer assembly and tubular packing both depend on the propeptide, D'D3 domains and acidic pH.[15, 30]

Recently, it has been demonstrated that the VWF C-terminals zip up and form a structure resembling a bouquet of flowers, where the A2, A3, and D4 domains comprise the flower part and the six VWC domains configure the stem. Dimeric bouquets are essential for correct VWF dimer incorporation into growing tubules and to prevent crosslinking between neighbouring tubules.[31, 32] Moreover, it was found that the last steps in VWF biosynthesis, interdimer N-terminal disulphide bond formation and cleavage by furin, appear to occur during or after assembly of individual VWF dimers onto the growing ends of tubules in nascent WPBs.[31] Helical assembly thus provides a template for disulphide bond formation during N-terminal concatamerization.[31] The lack of crosslinking between tubules promotes orderly unfurling of VWF from the ends of helices similarly to orderly uncoiling of a rope.[26] Dimeric bouquets are undoubtedly also important in compaction of WPBs during maturation and their expansion during secretion.[31]

Megakaryocytes synthesize large VWF multimers and package them into platelet α-granules that are spherical rather than cigar-shaped. The VWF multimers in α-granules are organized into clusters of tubules with dimensions similar to those of VWF tubules in Weibel–Palade bodies.[27, 30]

VWF secretion and catabolism

Secretion of stored VWF from endothelial cells occurs through both a constitutive and a regulated pathway.[2] The majority of endothelial-derived VWF is secreted via the constitutive pathway, which contributes to approximately 95% of plasma VWF; the remaining VWF is stored within WPBs of endothelial cells, and secreted via the regulated pathway on stimulation by secretagogues.[13] Megakaryocytes, however, lack the regulatory pathway, VWF is constitutively secreted and has not been shown to contribute significantly to plasma VWF.[2, 13]

It would be of great interest to define in detail the molecular mechanisms and machinery that underlie VWF secretion in health and disease.[33] In response to pathological stimuli, such as vascular injury and inflammation, the circulatory concentration of VWF increases rapidly mediated by secretagogues. The secretagogues can be divided into two distinct groups: Ca^{2+}-raising agonists (thrombin and histamine) and cAMP-raising agonists (epinephrine and vasopressin).[28, 33] In vivo, plasma VWF and FVIII levels rise rapidly after administration of the vasopressin analogue, 1-desamino-8-D-arginine-vasopressin (DDAVP), mediated by an increase in cAMP. The ability of DDAVP to raise plasma VWF and FVIII levels has made it a major drug for the treatment of VWD and hemophilia A.[3, 12]

Upon activation of endothelial cells by agonists, the WPBs fuse with the plasma membrane and release their contents into the blood circulation.[20, 33] During normal exocytosis, the shift in pH from pH 5.5 within the WPBs to the neutral pH of plasma leads to the unfolding of compact VWF tubules to VWF strings 100 times longer than the WPBs.[15, 26]

The length of the released VWF strings is typically several 100μm long but can reach extraordinary lengths of up to 1mm. These long VWF strings could arise through end-to-end self-association of VWF multimers.[34] Presumably, the unpaired cysteine thiols localized to the N-terminal D3 and C-terminal C domains are involved in VWF self association.[14, 35] Moreover, high shear stress changes the shape of the molecule from a globular form to an elongated or stretched form that is crucial for the interaction with platelets.[18]

The molecular size of VWF is critical for its physiologic function as a mediator of platelet adhesion and aggregation in primary hemostasis. The high-molecular-weight-multimers (HMWMs) are biologically most active and are essential to maintain hemostasis under conditions of high shear stress in the microvasculature.[36] However, the ultra large VWF (UL-VWF) is potentially harmful in the normal circulation and must be processed into smaller, less reactive molecules that will not precipitate unwanted platelet aggregation.[34] The highly pro-thrombotic UL-VWF is cleaved by the specific VWF cleaving protease ADAMTS13 (a disintegrin-like and metalloprotease domain with thrombospondin type-1 motif, number 13).[36] The ADAMTS13 cleavage site in

VWF (Met1605-Tyr1606) is normally hidden within the middle of the folded A2 domain.[34] High shear stresses can unfold the ADAMTS13 cleavage site in the A2 domain.[2]

The half-life of the circulating VWF multimers is ~ 12h.[12] It is demonstrated that macrophages and FVIII, mainly in the liver, mediate the removal of VWF from circulating blood. However, the precise cellular membrane receptors for VWF remain unknown.[2]

1.1.4 VWF functions

The VWF protein has three main recognized hemostatic functions, which are to mediate interactions of platelets to subendothelial matrix and platelets to platelets (platelet adhesion and platelet aggregation), and to serve as a carrier of factor VIII in the circulation system.[2] Recent studies have stated that VWF may have other, non hemostatic functions in angiogenesis, cell proliferation, inflammation, and tumor cell survival.[2, 14, 37]

Interactions between VWF and the subendothelial matrix

VWF performs a bridging function by binding the platelets to the extracellular matrix at sites of vascular injury.[3] When vessel wall subendothelium is exposed, VWF binds to collagen in the subendothelial matrix. The high shear stress allows conformational changes within VWF, which can result in the exposure of binding sites for platelets or collagen.[2, 34] The A1 domain of VWF interacts mainly with collagen type VI but can also bind, with less affinity, to collagen types I and III. The A3 domain can also bind to collagens, namely collagen types I and III.[2]

Role of VWF in platelet adhesion and aggregation

Under physiological conditions, circulating platelets are recruited from the blood flow to injury sites, where they act to prevent excessive bleeding. The highly polymerized VWF molecules are required to achieve efficient platelet adhesion

and aggregation.[17] The plasma VWF adheres to circulating platelets through two membrane receptors: glycoprotein Ib (GPIb) and the glycoprotein IIb–IIIa (GPIIb–IIIa) complex.[2,3] Upon exposure of vessel subendothelial matrix, VWF undergoes a conformational change after matrix binding and subsequently the binding site for the platelet receptor GPIb, located in the A1 domain of VWF, becomes accessible.

The platelet GPIIb/IIIa receptor only becomes available for VWF binding after platelet activation. Platelets are activated at sites of vascular injury by a variety of agonists. In addition, binding of VWF to the platelet GPIb receptor appears to activate platelets, making the GpIIb/IIIa receptor available for ligand binding. The RGD sequence near the C-terminus of VWF seems to be responsible for VWF binding to GpIIb/IIIa.[3]

GPIb participates mainly in platelet-vessel wall adhesion, while the GPIIb–IIIa complex is involved in both platelet-vessel wall adhesion and crosstalk between platelets. VWF is the only ligand that promotes platelet adhesion by attaching to both of these receptors.[2] Addition of a second layer of platelets (aggregation) involves binding of VWF to the GPIb and GPIIb/IIIa platelet receptors and of fibrin to GPIIb/IIIa. This results in forming a layer of VWF and fibrin coating the adhered platelets which functions as a platform for recruiting more circulating platelets. The aggregation of platelets continues until the injury is sealed off and a stable platelet plug has been formed.[38]

Carrier of factor VIII

VWF forms a complex with FVIII in plasma through a non-covalent interaction.[3] FVIII is a cofactor of the intrinsic clotting cascade, and its deficiency manifests as hemophilia A. VWF protects FVIII from degradation and may also serve to localize FVIII to the site of the clot. This phenomenon may be mediated by one or a combination of the following mechanisms: (1) structural stabilization of FVIII; (2) inhibition of phospholipid-binding proteins that target FVIII for proteolytic degradation; (3) inhibition of FVIII binding to activated FIX to stimulate the coagulation pathway, and (4) prevention of FVIII cellular uptake via scavenger cell receptors.[2]

FVIII binds to VWF within the N terminal of D' and D3 domains of VWF corresponding to residues 763-1035.[39]

1.2 VWD

Von Willebrand disease (VWD) is the most common inherited bleeding disorder. VWD has a prevalence of about 1% in the general population, but only approximately 1 in 10,000 individuals has clinically significant bleedings.[1, 40] VWD was first described in 1926 by Erik von Willebrand in a Finnish medical journal.[40] He described a young woman who bled to death at the time of her fourth menstrual period. Since then, significant advances in clinical and laboratory phenotypic description of patients and understanding of genetics of VWD has increased our knowledge on this disorder and its pathophysiology.[16, 40] However, the molecular basis of VWD remains the subject of ongoing investigations.[7]

VWD is caused by quantitative and/or functional deficits of VWF.[16] Characteristic bleeding symptoms include frequent nose bleeding, easy bruising, oral cavity bleeding, menorrhagia, bleeding after dental extraction, surgery, and childbirth.[7] Patients with severe forms of VWD may also suffer from joint, muscle and central nervous system bleeding.[16]

VWD has been classified into three primary categories. Types 1 and 3 VWD represent quantitative variants; type 1 VWD is a partial quantitative deficiency and type 3 VWD is a virtually complete quantitative deficiency of VWF. Type 2 VWD is characterized by a qualitative deficiency and defective VWF and is further classified into the four types 2A, 2B, 2M, and 2N.[7, 18] The functional defects lead to enhanced (2B) or reduced (2A, 2M) platelet interaction or impaired binding to FVIII (2N).[1] Generally, type 1, type 2A, type 2M and type 2B VWD are inherited in an autosomal dominant pattern, while type 3 and type 2N VWD are inherited in an autosomal recessive pattern.

1.2.1 Diagnosis and classification

The diagnosis and classification of VWD requires a combination of patients' medical history, specialized laboratory tests which can determine quantitative or qualitative defects in VWF and genetic testing.[18, 41] The correct classification of VWD facilitates the treatment and counseling of patients with VWD. In practice, distinctions between certain VWD types are not always easy to make.[42]

Bleeding history

A standardized bleeding history of the patient is a prerequisite for proper diagnosis of a patient with presumed VWD. This may be carried out by a standard questionnaire.[43] In addition, the utility of standard clinical assessment tools like bleeding severity score (BSS) to quantify bleeding symptoms facilitates diagnosis.[7] The BSS is a summary score from -3 to 45, based on the presence of various types of bleedings.[41]

Laboratory testing

For patients suspected of having a bleeding disorder, a number of laboratory tests may be necessary for proper diagnosis. Initial standard tests include activated partial thromboplastin time (aPTT), FVIII activity (FVIII:C), bleeding time and platelet function analyzer 100 (PFA100) assay. The specific assays important for VWD diagnosis are VWF antigen (VWF:Ag) determination, VWF:Ristocetin Cofactor activity (VWF:RCo), VWF:collagen binding (VWF:CB) and VWF:GPIb binding (VWF:GPIb).[18, 44] If abnormal results are obtained, specific assays should be performed to determine the subtype of VWD, such as multimer analysis, RIPA **(**Ristocetin induced platelet aggregation), VWF:FVIIIB (binding of FVIII to VWF) assay, and if indicated, molecular testing.[6, 7, 18]

VWF antigen (VWF:Ag): Quantity of VWF protein (antigen) in the plasma, measured antigenically using enzyme-linked immunosorbent assay (ELISA) or latex immunoassay. The normal range that should be determined independently by each laboratory is approximately 50–200 IU/dL.[7]

Ristocetin cofactor activity assay (VWF:RCo): This assay determines the ability of plasma VWF to interact with platelet GPIb, initiated by the antibiotic ristocetin. The normal range is approximately 50–200 IU/dL.[7]

Collagen binding assay (VWF:CB): This test determines the ability of VWF to bind to collagen (a subendothelial matrix component). The normal range is approximately 50–200 IU/dL.[7]

FVIII activity (FVIII:C): Functional FVIII assay that determines the activity of FVIII in the coagulation cascade. The normal range is approximately 50–150 IU/dL.[7]

VWF multimer analysis: SDS-agarose gel electrophoresis is used to determine the distribution of VWF oligomers in the plasma. High-resolution agarose-gel electrophoresis demonstrated that circulating VWF has a complex multimeric structure (Figure 1.3). The multimeric pattern of VWF that is seen on SDS/agarose-gel electrophoresis consists of regularly spaced bands while each band exhibits a triplet structure appearance. The smallest detectable subunit is a dimer with a molecular mass of ~540 kDa. The largest molecules exceed 10,000 kDa. The triplet bands of VWF are composed of mature, central band, and cleaved subunits by ADAMTS13 represented by a faster migrating satellite band and a slower migrating satellite band (Figure 1.3).[5, 45, 46]

Ristocetin induced platelet aggregation (RIPA): The RIPA test evaluates the ristocetin-induced aggregation of platelet-rich plasma. It is used to identify patients with type 2B and discriminates patients with type 2 VWD from those with type 1 VWD.[43]

Binding of FVIII to VWF (VWF:FVIIIB): This test that determines the ability of VWF to bind FVIII is useful for the identification and differential diagnosis of type 2N VWD.

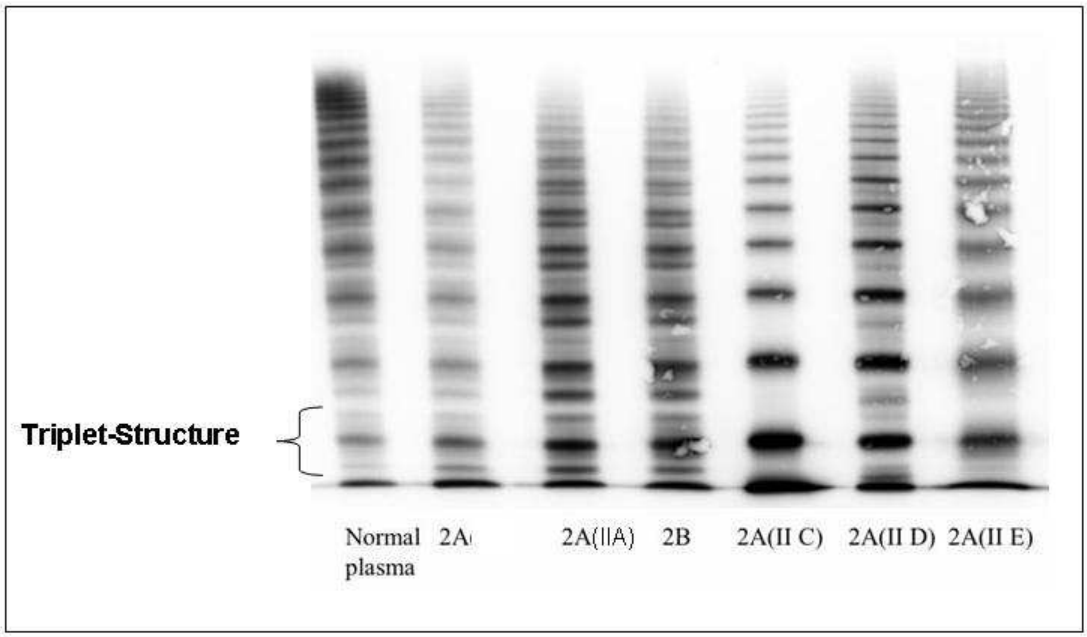

Figure 1.3. **VWF multimer patterns in normal plasma and different variants of type 2 VWD.** VWF multimers were separated by SDS gel electrophoresis and visualized by immunostaining. The triplet structures include central band and 2 flanking subbands. The image is adapted from the ISTH SSC VWD homepage.

Molecular genetic analysis

Molecular genetic analysis of patients is useful to further categorize VWD, and numerous mutations in the gene encoding VWF have been identified that correlate with specific subtypes of VWD.[18]

Classification

The International Society on Thrombosis and Haemostasis Scientific and Standardisation Committee (ISTH-SSC) on VWF provide recommendations for classification of VWD patients in 1994, and updated in 2006. [42] Table 1.1 summarizes the classification of VWD based on ISTH-SSC VWF guidelines.

VWD Type	Description
1	Partial quantitative deficiency of VWF Reduction of VWF:Ag, VWF:Ag/VWF:RCo>0.6, normal VWF multimer structure
2	Qualitative defects of VWF
2A	Decreased VWF-dependent platelet adhesion Associated with deficiency of HMW-multimers, VWF:Ag/VWF:Rco<0.6.
2M	Decreased VWF-dependent platelet adhesion. VWF:Ag/VWF:Rco<0.6 and/or reduced VWF:CB, and normal VWF multimer pattern
2B	Increased affinity for platelet GPIb; Characterized by increased RIPA at low ristocetin concentrations, and deficiency of HMW-multimers
2N	Markedly decreased binding affinity for FVIII (reduction in VWF:FVIIIB).
3	Virtually complete deficiency of VWF VWF:Ag <5 IU/dL and FVIII:C<10 IU/dL.

Table 1.1. Classification of VWD (adapted from Sadler JE, *et al.*)[42]

1.2.2 Characterization of VWD subtypes

VWD type 1

Type 1 VWD is the most common form of the disorder and accounts for up to 70% of all VWD. A VWF level less than 30–40 IU/dL indicates type 1 VWD.[18] However, it can be difficult to diagnose due to factors influencing VWF levels in plasma including environmental and genetics factors.[47] One of the major determinants of plasma VWF:Ag levels is the ABO blood group of an individual.[13, 48] ABO blood group O has been known to be more prevalent in type 1 VWD than in the normal population and is associated with VWF levels approximately 25% lower than the population average. The effect of blood-

group O appears to be due to increased VWF clearance from plasma; A and B blood-group glycosylation protects VWF from clearance,.[1, 49, 50]
The potential pathogenetic mechanisms characterized in type1 VWD to date include impaired biosynthesis, clearance (decreased survival) and intracellular retention of VWF.[51]

VWD Type 2

Type 2 VWD accounts for approximately 25% of all VWD.[7] Type 2 VWD is characterized by qualitative VWF deficiency. Levels of VWF:Ag may be decreased, normal or even elevated, but structural or functional defects lead to impaired activity.[16] Many type 2 VWD phenotypes can be distinguished from VWD type 1 by their decreased ratios of functional parameters, i.e. VWF:RCo, VWF:CB, VWF:GPIbB, VWF:FVIIIB, respectively, to VWF:Ag. Type 2 VWD subtypes include types 2A, 2B, 2M and 2N.[51] However, reliable classification of patients with VWD types 2A, 2B and 2M additionally requires multimer analysis.[16]

Type 2A VWD is the most common form of type 2 VWD which is associated with reduced platelet binding due to significant reduction or absence of VWF HMWM.[16] The hallmark of type 2A disease is a low VWF:RCo to VWF:Ag ratio (< 0.6) and impaired RIPA.[52] Four different subtypes of VWD type 2A including IIA, IIC, IID, IIE can be distinguished by multimer analysis indicating different underlying mechanisms (Figure 1.3).[1, 16] Type 2A (IIA) VWD results from mutations located in the A1 and A2 domains, which cause intracellular retention of HMWM (Group I) or enhanced susceptibility to ADAMTS13 cleavage (Group II). Type 2A VWD can also be caused by mutations interfering with multimerization assembly which either located in multimerization region (IIC and IIE) or in dimerization region (IID).[53, 54]

In type 2M VWD, platelet adhesion is defective despite a normal multimeric structure of VWF. The reduced capability for platelet adhesion is reflected by a low level of VWF:RCo or/and VWF:CB.[53, 55] Type 2M VWD typically results from

mutations disrupting binding of VWF to platelets (in A1 domain) or impairing collagen binding (mostly in A3 domain).[53]

Type 2B VWD is due to a gain-of-function mutation associated with increased affinity for platelet GPIb.[52] Although patients with type 2B VWD show loss of HMWM like type 2A VWD patients (Figure 1.3), they can be diagnosed phenotypically by enhanced RIPA at low concentration of ristocetin. In patients with classic type 2B, development of thrombocytopenia may occure during stressful situations, such as severe infection, surgery or pregnancy.[1] Type 2B is the result of missense substitutions in the GPIb binding region of VWF, the A1 domain.

Type 2N VWD ('N' for Normandy) represents forms of the disease with defective VWF:FVIII binding,thereby mimicking haemophilia A.[16] Symptoms largely result from reduced FVIII levels. VWF:RCo and VWF:Ag levels can be within the normal range, while FVIII:C is typically 5–40 IU/dL.

VWD Type 3

Type 3 VWD is the most severe and infrequent form of the disease,[55] and accounts for <5% of VWD patients.[7] Type 3 VWD is identified by VWF:Ag levels< 1% and moderate deficiency of FVIII (levels <10%).
It is an autosomal-recessive form of the disease due to homozygosity or compound heterozygosity of two mutations resulting in lack of VWF expression. In most cases, heterozygous mutation carriers of VWD type 3 are unaffected.[16] Phenotypic analysis is generally sufficient for diagnosis of the disorder, although molecular analysis can be useful where carrier status determination or prenatal diagnosis is required.

1.2.3 Treatment

The most important treatment options available for patients with VWD include stimulating the release of VWF from endogenous storage organelles by DDAVP, or replacement with plasma-derived VWF/FVIII concentrates.[16, 53, 56]

Other treatments that can reduce symptoms include fibrinolytic inhibitors and hormones for menorrhagia.[7]

DDAVP induces a prompt two- to fourfold increase in VWF plasma concentration and has therefore a significant role in the prevention and treatment of bleeding episodes in patients with VWD. The effectiveness of DDAVP is very variable between patients and dependent on the type of genetic defect in VWF.[28] Stimulation of endogenous VWF with DDAVP usually works well in patients with type 1 VWD.[53] Response to DDAVP among patients with type 2 VWD is heterogenous. In general, most type 2 patients produce dysfunctional VWF, so increasing levels of dysfunctional endogenous VWF with DDAVP might not be a viable strategy. Specifically, patients with type 2B VWD are usually not treated with DDAVP due to the occurrence of severe thrombocytopenia.[16] DDAVP is not effective in patients with type 3 VWD because these patients cannot produce any VWF. Type 3 VWD patients must be treated with VWF-containing concentrates.[57]

Therefore, the determination of correct subtype of VWD is important for selecting the available treatment options.

1.3 Aim and outline of the thesis

Diagnosis and classification of VWD can be complex because of variability in clinical manifestation and considerable heterogeneity in its molecular basis. Increasing our knowledge of the molecular biology and etiology of VWD will allow improvements in diagnosis, classification and consequently treatment of VWD patients. The main aim of the study was expanding our understanding of the molecular basis of different types of VWD to establish phenotype-genotype correlations. In addition, we aimed to elucidate the pathophysiological mechanisms of novel cysteine missense mutations within C-terminal domains of VWF which cause quantitative or qualitative VWD.

In chapter 2, we explored genotype and phenotype characteristics of a cohort of patients with VWD with the aim of dissecting the distribution of mutations in different types of VWD and correlate them to the clinical disease severity.

Moreover, the pathogenicity of novel candidate missense mutations and potential splice site mutations was predicted by *in silico* assessments.

In chapter 3, the presence of large deletions in *VWF* was investigated by multiple ligation-dependent probe amplification (MLPA), a gene dosage-based analysis method. The large deletions are likely to be missed by direct sequencing of *VWF* gene, where a heterozygous deletion is masked by the presence of an intact second allele. The MLPA analysis was performed for patients in whom no causative mutation was found, or homozygous causative gene alterations together with homozygous known polymorphisms were identified.

In chapter 4, the impact of five novel cysteine missense mutations residing in D4-CK domains on conformation and biosynthesis of VWF was characterized. These variants were identified as heterozygous in type 1 (p.Cys2619Tyr and p.Cys2676Phe), type 2A (p.Cys2085Tyr and p.Cys2327Trp) and as compound heterozygous in type 3 (p.Cys2283Arg) VWD. The effects of mutations on the processing of VWF including multimer assembly, its storage in Weibel-Palade bodies and secretion have been studied by transient expression in mammalian cell lines. Possible structural impact of these cysteine mutations was additionally studied by homology modeling.

Chapter 2

Mutation distribution in the von Willebrand factor gene related to the different von Willebrand disease (VWD) types in a cohort of VWD patients

Adapted from

Yadegari H., Driesen J., Pavlova A., Biswas A., Hertfelder H.-J., Oldenburg J.

Thrombosis and Haemostasis. 2012;108: 108(4):662-671

2.1 Abstract

In this study we explored genotype and phenotype characteristics of patients with VWD with the aim of dissecting the distribution of mutations in different types of VWD. One hundred fourteen patients belonging to 78 families diagnosed to have VWD were studied. Mutation analysis was performed by direct sequencing of the *VWF*. Large deletions were investigated by MLPA analysis. The impact of novel candidate missense mutations and potential splice site mutations was predicted by *in silico* assessments. We identified mutations in 66 index patients (IPs) (84.6%). Mutation detection rate was 68%, 94% and 94% for VWD type 1, 2 and 3, respectively. In total, 68 different putative mutations were detected comprising 37 missense mutations (54.4%), 10 small deletions (14.7%), 2 small insertions (2.9%), 7 nonsense mutations (10.3%), 5 splice-site mutations (7.4%), 6 large deletions (8.8%) and 1 silent mutation (1.5%). Twenty six of these mutations were novel. Furthermore, in type 1 and type 2 VWD, the majority of identified mutations (74% vs 88.1%) were missense substitutions while mutations in type 3 VWD mostly caused null alleles (82%). Genotyping in VWD is a helpful tool to further elucidate the pathogenesis of VWD and to establish the relationship between genotype and phenotype.

2.2 Introduction

Correct diagnosis and classification of VWD is important to provide the best therapeutic approaches to these patients.[18] However, diagnosis and classification of VWD can be complex because of clinical and laboratory variability and considerable heterogeneity in its molecular basis.[43] VWF plasma levels are affected by both inherited and acquired factors as ABO blood group, age, illness, pregnancy, and medication, making diagnosis of VWD, particularly type 1, difficult.[43, 58-61] On the other hand, in some occasions, compound heterozygosity for *VWF* mutations, or presence of mutations in the multifunctional domains of the VWF molecule cause pleiotropic effects and produce unique phenotype characterizations. Previous studies have demonstrated the challenge for a clear discrimination between type 1, 2A and 2M because of the overlap of these types.[62-64] Molecular genetic analysis in the last two decades has greatly enhanced our knowledge of the molecular biology of the disorder allowing improvement in diagnosis and management of patients with VWD. More than 500 different mutations are reported until now in the *VWF* database.[1] Nevertheless, for each of the three VWD types important clinical and biologic questions currently remain unanswered. Expanding our understanding of the molecular basis of VWD helps to find out the pathophysiological mechanisms of VWF mutations that will allow a more refined classification of VWD and establishment of phenotype-genotype correlations in the future.

In this study we explored genotype and phenotype characteristics of 114 patients with VWD with the aim of dissecting the distribution of mutations in different types of VWD and correlate them to the clinical disease severity.

2.3 Materials and Methods

2.3.1 Patients

A total of 114 patients belonging to 78 families from the Bonn Haemophilia Center (80% of patients) and also centers from different regions of Germany (20% of patients) with different types of VWD were recruited in our study. The patients were classified after laboratory and clinical investigation by the treating physician based on ISTH-SSC VWF guidelines.[42] Informed consent according to the declaration of Helnsinki was obtained from all index patients (IPs) and their family members. The majority of individuals collected for this study recorded their race/ethnic origin as Caucasian. Whole blood samples from IPs and their available family members were collected in both sodium citrate and EDTA tubes.

2.3.2 Phenotypic analysis

Coagulation assays: VWF antigen levels were measured using a particle-based turbidimetric assay, and procoagulant FVIII:C by an in-house clotting assay. Both assays were performed on a BCS XP coagulation analyzer according to the manufacturer's instructions (Siemens Healthcare, Marburg, Germany). The VWF:RCo assay and RIPA in platelet-rich plasma with final concentrations of ristocetin of 0,5 mg/ml and 1,2 mg/ml were performed using aggregometry-based in-house assays. The VWF:FVIIIB assay was performed at the source clinic attended by the patient.

Multimer assay: VWF multimer composition was evaluated by sodium dodecyl sulfate agarose gel electrophoresis followed by Western blotting and detection with rabbit anti-human VWF antibody (Dako, Glostrup, Denmark). The multimers were then visualized by luminescence (FluorChem 8000; Alpha Innotech Corp, Ca, USA).[65]

2.3.3 *VWF* analysis

DNA isolation: Genomic DNA was isolated from peripheral whole blood by standard salting out procedure. DNA purity and concentration were determined and standardized to 100 ng/µl.[66]

DNA sequencing: Fifty-six primer pairs were used to amplify *VWF*, including exons 2 to 52 and exon/intron boundaries. The promoter region and exon 1 were also investigated by 8 primer pairs in IPs without any clear causative mutation. DNA sequencing was performed on both strands, using the BigDye Terminator Cycle Sequencing V1.1 Ready Reaction kit and an automated ABI-3130 DNA sequencer (Applied Biosystems, CA, USA). Sequence Analysis software package (Applied Biosystems, CA, USA) was applied for final sequence reading and mutation documentation.

Any *VWF* sequence variation that was identified was noted. The ISTH SSC VWD homepage (http://vwf.group.shef.ac.uk/index.html accessed May 2012), VWFdb Hemobase (http://www.vwf.hemobase.com accessed May 2012) and the published literature were checked to see if the variation had been previously recorded and if the molecular mechanisms had been elucidated. SNPdb was checked for presence of novel substitutions through NCBI (http://www.ncbi.nlm.nih.gov/SNP accessed May 2012). We evaluated the likelihood that novel candidate missense mutations could be pathogenic with **S**orting **I**ntolerant **F**rom **T**olerant (SIFT, http://sift.jcvi.org accessed January 2011),[67] **Poly**morphism **Phe**notyping (PolyPhen, http://genetics.bwh.harvard.edu/pph accessed January 2011), and Align GVGD (http://agvgd.iarc.fr/agvgd_input.php accessed May 2012). Four splice site prediction software programs, Neural Network (http://www.fruitfly.org/seq_tools/splice.html accessed January 2011), NETGENE2 (http://www.cbs.dtu.dk/services/NetGene2/ accessed January 2011), WebGene Splice View (http://zeus2.itb.cnr.it/%7Ewebgene/wwwspliceview.html accessed May 2012), and MaxEntScan (http://genes.mit.edu/burgelab/maxent/Xmaxentscan_scoreseq_acc.html accessed May 2012) were used to investigate the possible pathogenicity of potential splice site mutations.

MLPA: Investigation for large deletions was performed by MLPA for patients without clear causative mutations. Patients were analyzed by MLPA (Kit P011 and P012, MRC Holland, Amsterdam, The Netherlands) according to the manufacturer's instructions.[68]

2.3.4 Structure analysis of VWF

The crystallographic models of the recombinant human VWF A2 domain (resolution solved to 2.3Å) and the A1 domain/GPIb complex (resolution solved to 3.1Å) were downloaded from the Protein Data Bank for viewing, analysis and graphical rendering using UCSF Chimera 1.2306.[69-71] Ribbon models were rendered with the A1/GPIb and A2 domains in different colors. The A1/GPIb complex is represented in bicoloured ribbons, the A1 domain turquoise colored and the Gp1b domain red colored. The side chains of the native residues at the positions of the reported human mutations were depicted as van der Waals spheres or sticks. Hydrogen bonds were inferred using the H-bond distance calculation algorithm of Mills & Dean (1996) relaxing constraints by 0.4 angstroms and 20 degrees.[72]

2.4 Results

One hundred fourteen patients belonging to 78 families were investigated in this study. Twenty-eight IPs with low VWF levels met the initial type 1 VWD diagnostic criteria according to ISTH-SSC VWF guidelines. The phenotypic characteristics of 32 IPs were in agreement with type 2 VWD of which 18 were assigned as type 2A, 7 as type 2M, 3 type 2B and 4 type 2N VWD. Eighteen IPs were diagnosed with type 3 VWD.

We identified putative mutations in 66 IPs (84.6%). In total, 68 different mutations were detected comprising 37 missense mutations (54.4%), 10 small deletions (14.7%), 2 small insertions (2.9%), 7 nonsense mutations (10.3%), 5 splice-site mutations (7.4%), 6 large deletions (8.8%) (20) and 1 silent mutation (1.5%). Of these 68 gene variants, 26 variants (38%) are reported for the first time.

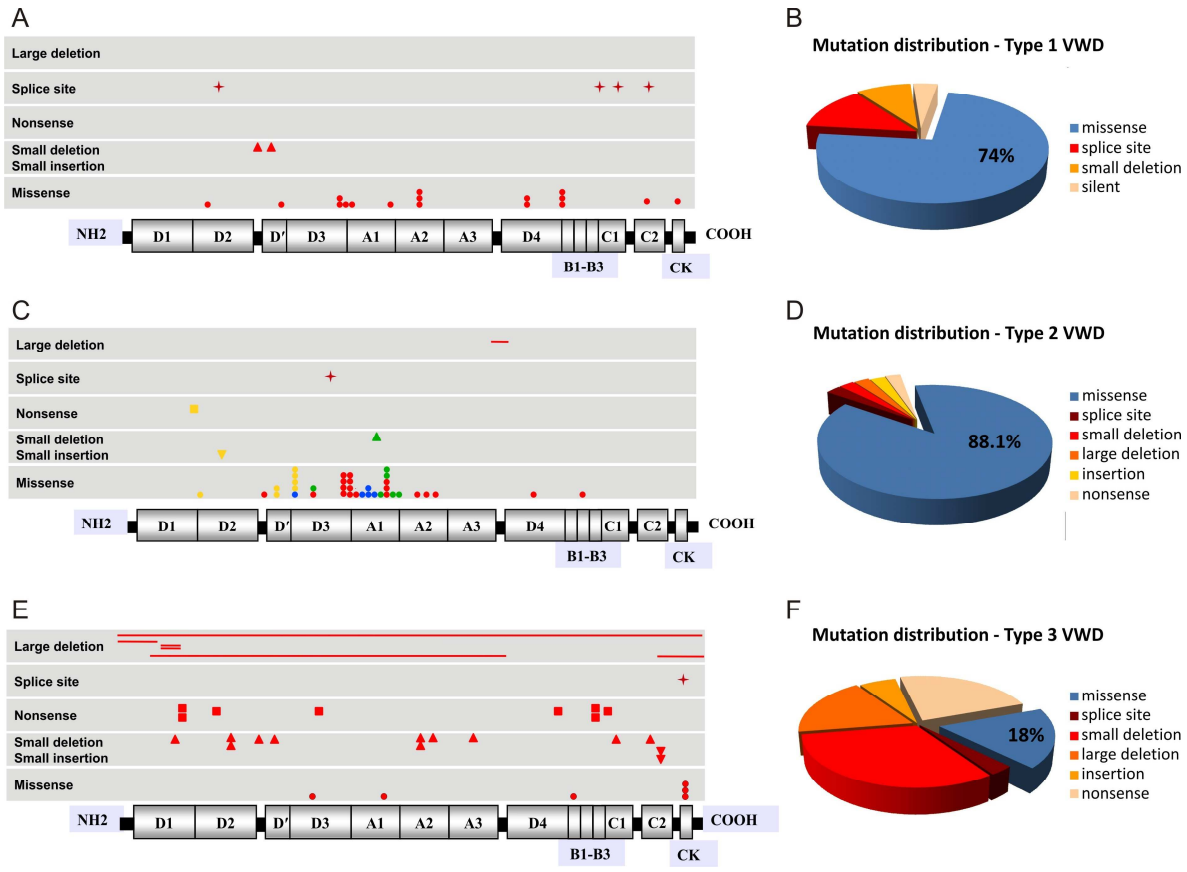

Figure 2.1. Mutation spectrum analysis of 78 families with VWD. Panels A, C and E show distribution of the mutations in relation to the functional domains of the VWF protein for type 1, type 2 and type 3 VWD, respectively. In Panel A, the silent mutation is considered as a splice site mutation. In Panel C, the mutations for each secondary category of type 2 are indicated by different colors, type 2A, type 2B, type 2M and type 2N mutations are shown in red, blue, green and yellow, respectively. Panels B, D and F show the type and frequency of mutations identified in type 1, type 2 and type 3 VWD of our cohort, respectively.
% represents the frequency of the missense mutations.

2.4.1 Mutations in Type 1 VWD

We identified *VWF* mutations in 19 (68%) of the 28 studied type 1 VWD patients. No *VWF* mutations were detected in 9 (32%) IPs, presenting with VWF:Ag level higher than 30%. In 3 (11%) IPs more than one putative mutation was identified. The mutations were distributed along all regions of the *VWF* (Figure 2.1A). However, a substantial number of candidate mutations was

clustered in exon 28 spanning the domains A1, A2, beginning of A3 and end of D3 domain.

A total of 23 putative mutations were identified in the type 1 VWD families (Table 2.1). The majority were missense mutations (n=17; 74%), of which 4 (p.Q499H, p.N857S, p.C2619Y and p.C2676F) are described for the first time (Figure 2.1B). Furthermore, 3 of these gene alterations (p.R1205H, p.Y1584C and p.S2179F) were repetitive and detected in more than 1 IP. In addition, 3 splice-site mutations, all affecting the donor splice sites, 2 common small deletions and 1 silent mutation were found in our cohort of type 1 VWD patients. Interestingly, the same small deletions were detected in type 3 VWD patients with another alteration assigning the type 3 VWD (Tables 2.1, 2.3).

Patients	Mutation Type	Nucleotide exchange	aa. Exchange	Domain	VWF:Ag %	VWF:Rco %	FVIII:C %
1	Missense	c.1497G>C§	p.Q499H	D2	44	33	54
1	Splice site	c.1533+1G>T		D2	60	51	83
1	Small deletion	c.2435delC	p.P812Rfs*31	D'	43	**	96
1	Missense	c.2570A>G§	p.N857S	D'	56		48
2	Missense	c.3614G>A	p.R1205H	D3-A1	15, 10	10,10	15,9
1†	Missense	c.3686T>G	p.V1229G	D3-A1	59	52	60
	Missense	c.3692A>C	p.N1231T	D3-A1			
1	Missense	c.4238C>T	p.P1413L	A1	44	50	55
2	Missense	c.4751A>G	p.Y1584C	A2	49, 38	42, 30	22,46
3	Missense	c.6536C>T	p.S2179F	D4-B	20,20,16	14,14,10	26,11,17
1	Silent	c.7464C>T§	p.G2488	C1	11	8	17
1	Splice site	c.7729+5G>A§		C2	65	52	79
1	Missense	c.7856G>A§	p.C2619Y	C2	37	43	
1	Missense	c.8027G>T§	p.C2676F	CK	29	22	58
1Nk	Small deletion	c.2269-2270delCT	p.L757Vfs*22	D2-D'	9	4	
	Splice site	c.7437+2T>C§		B3-C1			
1	Missense	c.4751A>G	p.Y1584C	A2	77	60	119
	Missense	c.6187C>T	p.P2063S	D4			
	Missense	c.6187C>T	p.P2063S	D4			

Table 2.1: Laboratory and genetic data of IPs with type 1 VWD.
The putative mutations marked with § are novel.
† indicates if 2 mutations are on the same allele; ‡ indicates if they are on two different alleles and NK if it is not known.
**: This patient is classified based on collagen binding value (CB: 43%).

2.4.2 Mutations in type 2 VWD

Different types of mutations were found in 30 out of 32 type 2 VWD IPs (93.7%). In two IPs, diagnosed with type 2A and type 2M based on laboratory data, no mutation in *VWF was detected*. In total, 27 different *VWF* variants were identified (Table 2.2). The majority (88.1%) of candidate mutations were missense substitutions (Figure 2.1D). Six of them (p.R854Q, p.R924Q, p.Y1146C, p.C1225G, p.R1306W and p.R1374H) occurred repetitively (Table 2.2). Missense mutations causing type 2A were predominantly clustered in exon 28 (Figure 2.1C). Interestingly, we report for the first time two novel missense substitutions in domain D4 and B (p.C2085Y and p.C2327W, respectively) causing type 2A VWD (Figure 2.1C). Additionally, 1 splice site mutation and 1 novel large deletion were detected in our cohort of type 2A VWD patients.

All mutations (6 previously reported missense mutations and 1 novel in-frame small deletion) causing type 2M VWD in our cohort of patients were located in domain A1 (Figure 2.1C) with the exception of mutation p.R924Q located in domain D3. Two of 3 type 2B IPs had 2 different mutations. One of them was compound heterozygous for the frequently described mutation p.I1309V and the novel substitution p.P1240L, and the other IP was compound heterozygous for mutations p.R1306W and p.R854Q showing a combined type 2B and type 2N phenotype. The missense mutation p.R854Q was detected in all patients with type 2N (either homozygous or compound heterozygous) except for one who was homozygous for the missense mutation p.T791M (Table 2.2).

Patients	Type 2 categories	Mutation Type	Nucleotide exchange	aa. exchange	Domain	VWF:Ag %	VWF:Rco %	FVIII:C %
4	2A	Missense	c.3437A>G	p.Y1146C	D3-A1	17-33	<10-18	21-32
1	2A	Splice site	c.3538+1G>A		D3	11	6	10
2	2A	Missense	c.3673T>G	p.C1225G	D3-A1	3	<6	5-35
	(atypical 2N)	Missense	c.3673T>G	p.C1225G	D3-A1			
1	2A	Missense	c.3863T>G	p.L1288R	D3-A1	33	15	30
1	2A	Missense	c.4571T>G[§]	p.V1524G	A2	90	25	45
1	2A	Missense	c.4789C>T	p.R1597W	A2	25	13	20
1	2A	Missense	c.4883T>C	p.I1628T	A2	20	8	39
1	2A	Large deletion	Exons 33-34 deletion[§]		A3-D4	17	9	1.9
1	2A	Missense	c.6254G>A[§]	p.C2085Y	D4	22	13	42
1	2A	Missense	c.6981T>G[§]	p.C2327W	B	13	7	22
1	2A	Missense	c.4121G>A	p.R1374H	A1	12	<6	27
1[NK]	2A	Missense	c.4121G>A	p.R1374H	A1	42	17	46
		Missense	c.2220G>A	p.M740I	D2-D'			
1[‡]	2A	Missense	c.4121G>A	p.R1374H	A1	39	<6	22
		Missense	c.2771G>A	p.R924Q	D3			
1	2B	Missense	c.3916C>T	p.R1306W	A1	50	26	57
1[NK]	2B	Missense	c.3916C>T	p.R1306W	A1	50	24	29
		Missense	c.2561G>A	p.R854Q	D'			
1[‡]	2B	Missense	c.3925A>G	p.I1309V	A1	75	56	55
		Missense	c.3719C>T[§]	p.P1240L	D3-A1			
1	2M	Missense	c.3943C>G	p.R1315G	A1	25	11	37
1[‡]	2M	Small Deletion	c.3964_3966delCAC[§]	p.H1322del	A1	21	8	19
		Missense	c.2771G>A	p.R924Q	D3			
1	2M	Missense	c.4120C>T	p.R1374C	A1	22	11	38
1	2M	Missense	c.4121G>T	p.R1374L	A1	20	7	20
1	2M	Missense	c.4105T>A	p.F1369I	A1	30	15	30
1	2M	Missense	c.4225G>T	p.V1409F	A1	27	<6	23

Patients	Type 2 categories	Mutation Type	Nucleotide exchange	aa. exchange	Domain	VWF:Ag %	VWF:Rco %	FVIII:C %
1	2N	Missense	c.2561G>A	p.R854Q	D'	75	108	40
		Missense	c.2561G>A	p.R854Q	D'			
1[NK]	2N	Missense	c.2561G>A	p.R854Q	D'	45	40	30
		Nonsense	c.970C>T	p.R324*	D1-D2			
		Missense	c.1001G>A[§]	p.G334E	D1-D2			
1[‡]	2N	Missense	c.2561G>A	p.R854Q	D'	38	43	9
		Insertion	c.1722_1723insVWFc.1682_1729+33[§]	p.P574_R575ins	D2			
1	2N	Missense	c.2372C>T	p.T791M	D'	124	96	3
		Missense	c.2372C>T	p.T791M	D'			

Table 2.2: Laboratory and genetic data of IPs with type 2 VWD.
The putative mutations marked with § are novel.
† indicates if 2 mutations are on the same allele; ‡ indicates if they are on two different alleles and NK if it is not known.

2.4.3 Mutations in type 3 VWD

We could detect mutations in 17 of 18 IPs (94.4%). All IPs except one were homozygous or compound heterozygous for given mutations (Table 2.3). In total, we identified 26 different *VWF* mutations in type 3 VWD families. The majority of mutations (82%) were null mutations (Figure 2.1F) resulting in severely decreased VWF:Ag levels. In total, we found 4 previously reported missense mutations, 5 large deletions (4 novel), 9 small deletions (5 novel), 1 insertion, 1 splice site mutation and 6 nonsense mutations (2 novel) (Figure 2.1E). All small deletions detected in our cohort caused a shift of the reading frame and determined a premature termination codon. The small deletions c.2435delC and c.7650-7651delCC were located in a stretch of cytosine residues while c.7524-7525delGG was in a stretch of guanine residues. One previously described cytosine insertion in a stretch of four cytosines (c.7671-7674) in exon 45 was detected (c.7674_7675insC) in a homozygous status.

Patients	Mutation type	Nucleotide exchange	aa exchange	Domain	VWF:Ag %	VWF:RCO %	FVIII:C %
1‡	Large deletion	*VWF*-del		all domains	<6	<6	2
	Small deletion	c.7650_7651delCC§	p.Q2551Afs*16	C2			
1	Large deletion	Exons 4-34 del§		D1-D4	<1	<6	2.4
1NK	Large deletion	Exons 1-5 del§		Signal-D1	1	5	1.4
	Missense	c.2771G>A	p.R924Q	D3			
1NK	Large deletion	Exons 48-52§		C2-CK	<3	<10	2.3
	Small deletion	c.2269_2270delCT	p.L757Vfs*22	D2-D'			
1	Large deletion	Exon 6 del§		D1	<1	<6	5
	Large deletion	Exon 6 del		D1			
1NK	Small deletion	c.1051delG§	p.V351Cfs*106	D1	<1	<6	2.4
	Splice site	c.8155+3G>A		CK			
1	Small deletion	c.1933_1945del§	p.P645Sfs*1	D2	1	<6	1.7
	Small deletion	c.1933_1945del	p.P645Sfs*1	D2			
	Nonsense	c.6490C>T§	p.Q2164*	D4			
1NK	Small deletion	c.2435delC	p.P812Rfs*31	D'	<1	<1	<1
	Nonsense	c.1659G>A	p.W553*	D2			
1	Small deletion	c.4570delG	p.V1524fs*	A2	3	<6	4
	Small deletion	c.4570delG	p.V1524fs*	A2			
1NK	Small deletion	c.4944delT	p.I1649Sfs*44	A2	<1	<6	4.4
	Missense	c.6911G>A	p.C2304Y	B			
1‡	Small deletion	c.5310delC§	p.I1770Mfs*121	A3	<3	<10	1.8
	Missense	c.4120C>A	p.R1374S	A1			
1	Small deletion	c.7524_7525delGG§	p.D2509Lfs*24	C1	<1	<6	3.7
	Missense	c.8216G>A	p.C2739Y	CK			
1NK	Small Insertion	c.7674_7675insC	p.S2559Lfs*8	C2	<1	<6	1.4
	Small Insertion	c.7674_7675insC	p.S2559Lfs*8	C2			
1	Nonsense	c.1093C>T	p.R365*	D1	1	<6	<10
	Nonsense	c.1093C>T	p.R365*	D1			
1NK	Nonsense	c.3360G>A§	p.W1120*	D3	4.7	4.5	
	Nonsense	c.7300C>T	p.R2434*	B3-C1			
1	Nonsense	c.7176T>G	p.Y2393*	B	3	<5	4
	Nonsense	c.7176T>G	p.Y2393*	B			
1	Missense	c.8216G>A	p.C2739Y	CK	3	<6	2
	Missense	c.8216G>A	p.C2739Y	CK			

Table 2.3: Laboratory and genetic data of IPs with type 3 VWD.

The mutations marked with § are novel.
† indicates if 2 mutations are on the same allele; ‡ indicates if they are on two different alleles and NK if it is not known.

2.4.4 Prediction of impact of novel substitutions

The predicted impact of the novel putative mutations was assessed by SIFT, PolyPhen, and Align GVGD. Obtained scores are summarized in Table 2.4. Both algorithms, SIFT and PolyPhen, showed that all novel missense changes, except two, are probably damaging. Align GVGD software predicted all novel

candidate missense mutations except three can most likely interfere with function of protein. The variants p.N857S and p.P1240L were assigned as tolerable by all three programs. The variant p.P1240L was additionally reported in SNPdb as a SNP detected in a normal population. The Align GVGD pointed the variation p.Q499H as less likely affective.

Two novel splice site mutations (c.7437+2 T>C and c.7729+5 G>A) were predicted to be deleterious by all four splice-site analysis tools. Moreover, the analysis of the silent mutation detected in exon 44 (c.7464C>T, p.G2488) showed that it might create a cryptic donor splice site (Table 2.5).

AA exchange	Domain	VWD Type	SIFT prediction	PolyPhen prediction	AGVGD Prediction
p.G334E	D1-D2	2N	Affect the P.F.	P. D.	Most likely IPF
p.Q499H	D2	1	Affect the P.F.	P.D.	Least likely IPF
p.N857S	D'	1	Tolerated	Benign	Least likely IPF
p.P1240L	D3-A1	2B	Tolerated	Benign	Least likely IPF
p.V1524G	A2	2A	Affect the P.F.	P. D.	likely IPF
p.C2085Y	D4	2A	Affect the P.F.	P. D.	Most likely IPF
p.C2327W	B	2A	Affect the P.F.	P. D.	Most likely IPF
p.C2619Y	C2	1	Affect the P.F.	P. D.	Most likely IPF
p.C2676F	CK	1	Affect the P.F.	P. D.	Most likely IPF

Table 2.4: Summary of in silico analysis (SIFT, Polyphen and Align GVGD) for novel candidate missense mutations.
P. F.: Protein function, P.D.: Probably damaging, IPF: Interfer with protein function.

Nucleotide Change	Neural Network native-mutated	NetGene2 nativ-mutated	MaxEntScan native-mutated	WebGene Splice View Native-mutated
c.7437+2 T>C	0.98-Native DSS destroyed	0.997-Native DSS destroyed (0.227)	11.11-3.36	88-Native DSS destroyed
c.7464 C>T (p.G2488)	No P.SS-New P.DSS (0.99)	No P.SS (0.849)-New P.DSS (1.000)	2.72-10.47	No P.SS-New P.DSS (94.)
c.7729+5 G>A	0.97-Native DSS destroyed	0.962-Native DSS destroyed (0.378)	8.37-3.86	86-79

Table 2.5: Summary of novel potential splice site mutations prediction.
DSS: Donor splice site. P.DSS: Potential donor splice site. P.SS: Potential splice site. The higher the score, the higher the probability that the sequence is a true splice site.

2.4.5 Structure analysis of four missense mutations located in A1 and A2 domains of VWF

Structural analysis was done for the novel mutation p.V1524G and 3 other recently reported, but not well functionally studied mutations - p.R1315G, p.V1409F and p.L1288R (Figure 2.2). Two mutations causing type 2M (p.R1315G and p.V1409F) and 1 causing type 2A (p.L1288R) were in domain A1, the domain interacting with GPIb receptor on platelets. Investigation of the local environment for these mutant residues identifies domain instability induced by side chain clashes/disruption of hydrogen bonds as their primary causative influence (Figure 2.2A-C). The mutations p.R1315G and p.V1409F also have a negative influence on the binding of A1 domain to the GPIb molecule. One other mutation, p.V1524G (causing type2A VWD) in the A2 domain, results in an easier access of the ADAMTS13 cleavage site by facilitating the unfolding of this domain (Figure 2.2D).

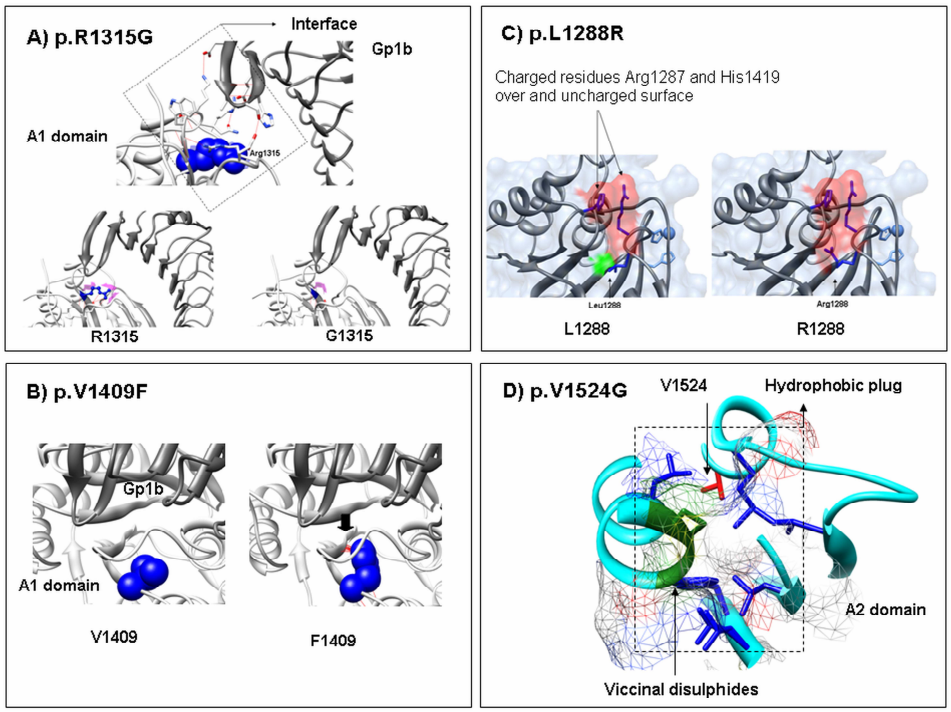

Figure 2.2. Close-up views of the local molecular environments of four human VWFA1 and VWFA2 domain missense mutations depicted on structural models of VWFA1 /GPIb and VWFA2 domains (PDB ID: 1M10; resolution: 3.10A° and PDB ID: 1AUQ; resolution: 2.30A° respectively).

The figure is divided up into four panels representing four different mutations. Panel A, B and C depict mutations in VWFA1 domain while Panel D corresponds to mutation in VWFA2 domain. Panel A. The panel is split into three images. The top image depicts the interface between the VWFA1 domain and GPIb molecule. The contacts (H-bonds) across the interface are represented by red lines. The affected residue is depicted as a dark blue CPK sphere. The image on the left shows the H-bonds formed by the wild type p.R1315 residue. The image on the right shows the H-bonds formed by the mutated p.G1315 residue. Both residues are depicted as ball and stick models. No structure is apparent for the side-chain of glycine since it is a single hydrogen atom (not resolved in the 3.10 Å X-ray crystallographic data). The backbone of the VWFA1 domain and GPIb molecule are represented as grey ribbons respectively. The effective surface of these residues is depicted in magenta. Panel B. The panel is split into two images. The image on the left shows the wild type p.V1409 residue and the image on the right shows the mutated p.F1409 residue. The backbone of the VWFA1 domain and GPIb molecule are represented as grey ribbons. The residues are represented as CPK spheres. The red lines which are indicated with a black arrow depict clashes with p.I617 and p.A618. Panel C. The panel is split into two images. The residues of interest are represented as dark blue sticks. The left image depicts local environment of the wild type p.L1288 residue. The positive charge on the residues proximal to the affected p.L1288 are represented in red surface colors while the neutral charge of the p.L1288 residue is depicted in green. The right image represents the mutated p.R1288 residue which brings another positive charge in proximity to the other two charged residues giving a reddish hue to the original green colored surface. Panel D p.V1524 (red sticks) is shown near the hydrophobic plug formed by the vicinal disulphides (green ribbon and stick) and 8 other hydrophilic residues (deep blue sticks). The backbone of the VWFA1 domain is represented as a turquoise ribbon.

2.5 Discussion

In the present cohort, we investigated VWD patients for variations within *VWF* to elucidate the molecular basis for each type in order to enhance understanding of the disorder. The majority of mutant alleles (74% vs 88.1%) identified in our patients with type 1 and type 2 VWD were missense mutations, while null alleles were predominant (82%) in patients with type 3 VWD (Figure 2.1 B, D and F). The sequence variants identified in our cohort of type 1 and type 3 VWD patients spread throughout the whole *VWF*, but as expected, were confined to a particular region of the *VWF* in the different types of our patients with type 2 VWD (Figure 2.1A, C and E). These findings are in line with previous reports.[1, 51, 73-75]

The VWF:Ag level was variable in our cohort of type 1 VWD patients. A mean VWF:Ag of 39.5% was registered, ranging from 9% to 77%. Our data showed a correlation between VWF:Ag level and mutation detection rate. In all patients with type 1 VWD and VWF:Ag level less than 30% mutations were identified. In contrast, in only 53% of patients a mutation was detected when VWF:Ag was higher than 37%. Our data supported the finding of other groups,[73, 74] indicating that in milder cases of VWD, the genetic determinants are more complex and might involve other factors outside the *VWF*. In our study, VWD type 1 patients bearing p.S2179F and p.R1205H expressed the lowest VWF antigen levels (10-20%) compared to the antigen levels of patients with other missense mutations. These data are in concordance with the literature.[62-64, 76, 77]

Although the pattern of mutations found in type 3 VWD patients was similar to previous studies, only few of the mutations identified so far have been found repetitively in analogous studies from different populations.[78-80] The presence of 11 novel mutations in 17 IPs diagnosed as type 3 VWD in our cohort shows a high degree of genetic heterogeneity in the molecular pathology of type 3 VWD.

VWD is known for a high degree of variability in clinical presentation and a considerable heterogeneity of its molecular basis. It has been shown that within the phenotypic classification of VWD, variations within a single mutation can be responsible for different types of the disease. Thus, some substitutions are discussed controversially. The missense mutations affecting p.R1374 is

presented with different variants depending on the nucleotide substitution. In our study the variant p.R1374H led to type 2A VWD. Two other variants of p.R1374, p.R1374L and p.R1374C, were considered to be responsible for type 2M VWD (Table 2.2). Although the ISTH registry of VWD assigns these variants as unclassified (U), they have been classified by several investigators into different VWD types due to the patient´s pleiotropic phenotype.[1, 75, 81-83]

In some cases an equal mutation contributes to expression of different phenotypes. The variant p.R924Q is listed as a polymorphism, as a type 2N mutation and also as a type 1 mutation in the ISTH SSC VWF database. In our study this gene alteration was associated with type 2M (2 patients) and type 3 (1 Patient) VWD. However, p.R924Q was found as a second causative mutation in a patient with type 3 VWD. Berber et al. demonstrated through *in vitro* expression studies that the p.R924Q variation does not significantly affect biosynthesis of VWF, but they suggested that this variant allele may mark a null allele in some instances.[84] Hickson et al also reported that its inheritance alone may be insufficient for VWD diagnosis, but it appears to be associated with a further VWF level reduction in individuals with a second *VWF* mutation.[85] Therefore, we cannot exclude the possibility of a second mutation in intronic regions or outside of the *VWF* for the IP with type 3 VWD.

The variant p.P2063S is listed in the ISTH SSC VWF database as a type 3 mutation, and it has been identified in Canadian and Spanish populations in type 1 VWD patients.[63, 82] Moreover, p.P2063S is found in a Spanish population in compound heterozygous state with p.V1409F in a type 2M patient with Blood group A, VWF:Ag 9% and VWF:RCo 3%.[82] The patient heterozygous for p.V1409F variant with Blood group A classified as type 2M in our cohort shows VWF:Ag 27%, VWF:RCo <6. Comparison of the laboratory data of these 2 patients indicates a possible influence of p.P2063S as a second variant for the quantitative defect in the Spanish patient. However, the functional study of this substitution by Eikenboom et al. showed that p.P2063S is possibly a polymorphism.[86] In our cohort, p.P2063S was detected in homozygous state in combination with p.Y1584C in a patient with type 1 VWD exhibiting VWF:Ag level of 77% and VWF:RCo of 60%. Since p.Y1584C is also known as a variant

with incomplete penetrance, determination of causative mutation explaining the phenotype of this patient is ambiguous.

An interesting mutation is p.C1225G listed as a type 2N mutation in the ISTH SSc database. In our cohort the patients carrying p.C1225G are classified as type 2A VWD owing to relative reduction of big multimers and normal values of VWF:FVIIIB (in one patient). However, Allen et al. classified this mutation as an atypical type 2N mutation.[87] They discovered by *in-vitro* expression of the recombinant VWF that this mutation affects the level of secreted VWF, the binding of VWF to factor VIII and the ability of VWF to form multimers. The pleiotropic effects of this mutation on the VWF molecule make its classification complicated.

The novel variant p.N857S is predicted to be benign by all predictive tools, but it is one of the twelve N-linked glycosylation sites of the mature VWF protein.[88] Therefore, its causality cannot be excluded prior to expression studies. In total, we found 5 splice site mutations and 1 silent mutation. The previous studies have proved the causality of 3 of these splice site mutations by mRNA analysis.[77, 89] Both, two novel splice site mutations and 1 novel silent mutation, were predicted to be causative by all splice-site analysis tools used in our study.

Structural interpretation

The A1 domain structure can be divided into six unique faces or fronts.[70] The p.R1315 residue is located on a beta strand from the previously defined “lower face”. It is part of an elaborate set of domain stabilizing salt bridge networks and forms hydrogen bonds with an adjacent strand and a loop. Mutation to a much smaller glycine residue would result in the disruption of these H-bonds resulting in domain instability (Figure 2.2A). Additionally, since the confirmation of this region is essential for binding to platelets, the altered domain structure would also negatively influence the same. The mutation p.V1409F is also situated in proximity of this surface and the resulting longer Phenylalanine side chain may result in side chain clashes and disturb the binding of this surface to the Gp1b molecule (Figure 2.2B). The mutation p.L1288R is located on the previously defined “upper face” of the A1 domain which is uncharged surface of approx.

20A° diameter with charged residues only at the periphery.[70] The only charged residues on this surface are the p.R1287 and p.H1419 (Figure 2.2C). The mutation of p.L1288 to a large positively charged arginine residue over this surface will destabilize this region and result in an unstable molecule. The mutation also disrupts a domain stabilizing salt bridge network (loss of H-bonds to a connecting loop and helix) resulting in an unstable A1 domain.

The shear induced unfolding of the VWF A2 domain to expose the p.Y1605-p.M1606 ADAMTS13 cleavage site, is a well investigated phenomena.[90] In the A2 domain crystal structure 3GXB, the p.V1524 residue is proximal to a hydrophobic plug formed by the hydrophobic interaction of the vicinal disulfides and eight residues which forms the first high energy barrier against the unfolding (entry of water molecule) of the A2 domain prior to the final rate limiting step (Figure 2.2D).[90] The mutant polar p.G1524 residue in the proximity of this hydrophobic plug will reduce the energy barrier for this step and result in easier access to the ADAMTS13 cleavage site.

In conclusion, our study extends the mutational spectrum of *VWF*, and improves the knowledge on the genetic basis of different types of VWD. This data provides the opportunity to possibly design functional studies to understand molecular mechanisms underlying this disease and establish genotype-phenotype correlations for proper classification and improving clinical management. Additionally, our study also shows that the combination of mutations causing different types of VWD within one patient causes complex phenotypes. Finally, the availability of well defined crystal structures for some of the VWF domains is useful in understanding the molecular etiology of some of the variants and their impact on protein structure. The understanding of the molecular etiology of these variants is crucial in determining their causality and therefore establishing their credentials as mutations or mere neutral polymorphisms.

Chapter 3

Large deletions identified in patients with von Willebrand disease using multiple ligation-dependent probe amplification

Adapted from

Yadegari H., Driesen J., Hass M., Budde U., ,Pavlova A., and Oldenburg J.

Journal of Thrombosis and haemostasis. 2011;9:1083-1086

3.1 Abstract

Large deletions are considered as being a rare cause of VWD. In the VWF database only 12 large deletions are reported ranging in size from a single exon to the entire gene. The aim of our study was screening for large deletions of *VWF* in VWD patients where direct sequencing of *VWF* failed to reveal causative VWF gene mutations or showed homozygousity for a given mutation and polymorphisms. Twenty-three patients were investigated, including 11 patients with type 1, 3 patients with type 2 and 9 patients with type 3 VWD. Genomic DNA was isolated by standard methods and investigation for large deletions was performed by MLPA. Six large deletions were identified in our cohort of which five were not previously described. Five large gene deletions were detected in patients with type 3 VWD and one in type 2 VWD. A homozygous deletion of exon 6 was identified in 2 patients with type 3 VWD belonging to the same family. The deletion segregates within the family and was detected in another four family members in heterozygous state. The deletions spanning the exons 1-5, whole gene and exons 48-52 were combined with a second mutation affecting the other allele – a missense mutation, a small deletion in exon 45, or a small deletion in exon 17, respectively. In the patient with the heterozygous large deletion of exon 4-34, no second mutation was identified. Interestingly a large deletion of exons 33-34 of *VWF* along with a missense mutation in FVIII gene (*F8)* was detected in a combined type 2A VWD/hemophilia A patient. Our results indicate that investigation for presence of heterozygous large deletions should be taken into consideration when no causative mutations are identified, or homozygous polymorphisms and homozygous mutations are detected.

3.2 Introduction

A large diversity of mutations as missense, nonsense and splice site mutations, small deletions/insertions and large deletions has been reported in the *VWF* gene database.[91] Large deletions are regarded as being a rare cause of VWD, usually resulting in a complete lack of VWF protein.[10] Twelve large deletions, ranging in size from a single exon to the entire gene, responsible for type 3 VWD are reported up to now. In some instances, large deletions represent a cause of both types of 1 and 3 VWD.[92] Interestingly, a large deletion covering all VWF A domains has been described for type 2A.[91] An Alu repeat-mediated unequal homologous recombination event is the most common mechanism involved in large deletions in the *VWF*.[55, 93, 94] There are approximately 100000 Alu repeats in the human genome, and these have been repeatedly involved in the generation of deletion mutations. At least 14 Alu sequences have been identified in *VWF .*[95]

Large deletions are particularly difficult to detect in autosomal conditions, where the failure to amplify one *VWF* allele can be masked by amplification of the second allele. Thus, false-negative results in carriers of heterozygous large deletions can be obtained. Methods based on gene dosage analysis such as MLPA have been successfully applied for detection of heterozygous deletions.[95] The aim of our study was to determine the molecular basis of VWD in patients, where direct sequencing of *VWF* gene failed to reveal causative mutations.

3.3 Method and materials

Seventy nine IPs with different types of VWD from the Bonn Haemophilia Center have been included in our investigation. All patients gave informed consent according to the declaration of Helsinki. Genomic DNA was isolated by standard methods. Mutational screening analysis was carried out by direct sequencing of exons 2 to 52 including exon/intron boundaries of the *VWF* gene for all patients with VWD. We could not detect causative mutations in 11 IPs with type 1 and in 3 patients with type 2 VWD, which were further investigated for the presence of large deletions. Patients with type 3 VWD, in whom no

mutation was found (1 patient), or a homozygous causative gene alteration together with homozygous known polymorphisms were identified (4 patients), as well as patients with only one heterozygous genetic defect discordant to the severity of the disease (4 patients) were additionally tested for the presence of a large deletion. All 23 patients were analyzed by MLPA (Kit P011 and P012, MRC Holland, Amsterdam, The Netherlands) according to the manufacturer's instructions. The PCR products were run on an ABI PRISM 3130XL sequencer with the GeneScan 500 LIZ size standard and analyzed by GeneMapper Software 5.0 (Applied Biosystems). Dosage analysis based on a comparison between deleted and reference wild-type DNA samples were performed by the Excel-based software Coffalyser V9.4 (MRC-Holland).

3.4 Results and Discussion

In total, 6 large deletions (5 novel) were identified in our cohort of patients with VWD. Five large gene alterations were detected in patients with type 3 VWD and one account for type 2 VWD (Table 3.1).

	vWF:Ag	vWF:RCo	FVIII:C	Allele 1			Allele 2	Type VWD
	(%)	(%)	(%)	Exon	aa substitution	Zygosity		
IP-1	<1	<6	5		Deletion exon 6	homozygous	Deletion exon 6	Type 3 VWD
IP-2	<6	<6	2	45	p.Gln2551AlafsX16	homozygous	Whole gene deletion	Type 3 VWD
IP-3	1	5	1,4	21	p.Arg 924Gln	heterozygou	Deletion exons 1-5	Type 3 VWD
IP-4	3			17	p.Leu 757ValfsX22	heterozygou	Deletion exons 48-52	Type 3 VWD
IP-5	<1	<6	2,4		No mutation		Deletion exons 4-34	Type 3 VWD
IP-6	17	9	1,9*		No mutation		Deletion exons 33-34	Type 2 VWD

Table 3.1. Laboratory phenotype and molecular genetic analyses of patients with VWD.

*= The patient IP-6 had an additional mutation in the *F8* (Asn2129Ser)

Our first patient presented with homozygous large deletion of exon 6, detected directly by lack of amplification product of exon 6 and confirmed by MLPA (Table 3.1, Figure 3.1A). This patient exhibited severe bleeding symptoms

subjecting him to prophylactic treatment. The serological measurements of VWF antigen (VWF:Ag) of <1%, VWF ristocetin-cofactor activity (VWF:RCo) of <6% and factor VIII activity (FVIII:C) of 5% confirmed the VWD type 3. The homozygous status of the deletion was due to the consanguineous marriage in the family. The deletion segregates within the family and was detected in another 6 family members – in 5 as a heterozygous gene defect and in one in homozygous state. All heterozygous family members showed reduced values of VWF:Ag ranging from 49% to 84%, VWF:RCo – 48-76% and FVIII:C 70-83%. All patients experienced mild bleeding symptoms such as epistaxis and cutaneous hemorrhages that meet the criteria of mild type 1 VWD. The sequencing results of *VWF* gene revealed a homozygous small deletion in exon 45 (p.Gln2551AlafsX16) of IP-2 (Table 3.1). As consanguinity was excluded and the laboratory data were susceptible to type 3 VWD (VWF:Ag <6%, VWF:RCo <6% and FVIII:C 2%), MLPA was performed (Table 3.1). A whole gene deletion was detected, which clearly explained the pseudo-homozygous presentation of the small deletion and corresponds to the type 3 VWD (Figure 3.1B). Clinically, repetitive severe epistaxis and subcutaneous haematomas were observed. The mother reported no history of bleeding episodes and the laboratory data were in the border line of the normal range. Only the heterozygous small deletion was proven after sequencing of the *VWF*.

The next two patients in our cohort (IP-3 and IP-4) presented with type 3 VWD due to compound heterozygous mutations. In the first case, a missense mutation (p.Arg924Gln) was combined with a large deletion spanning exons 1-5 (Table 3.1, Figure 1.3C). We expect the Arg924Gln and the large deletion to be compound heterozygous, because of the VWD type 3 phenotype and because no other mutation could be found. However, as no further relatives have been available to determine the phase, it cannot be excluded that both mutations are located on the same allele and a so far not detected mutation is affecting the second allele. Clinical data in this patient showed severe bleeding episodes including repetitive epistaxis, cutaneous and muscles haematomas, postpartum bleedings and a heavy menorrhagia, subjecting her to a prophylactic treatment.

A. IP-1

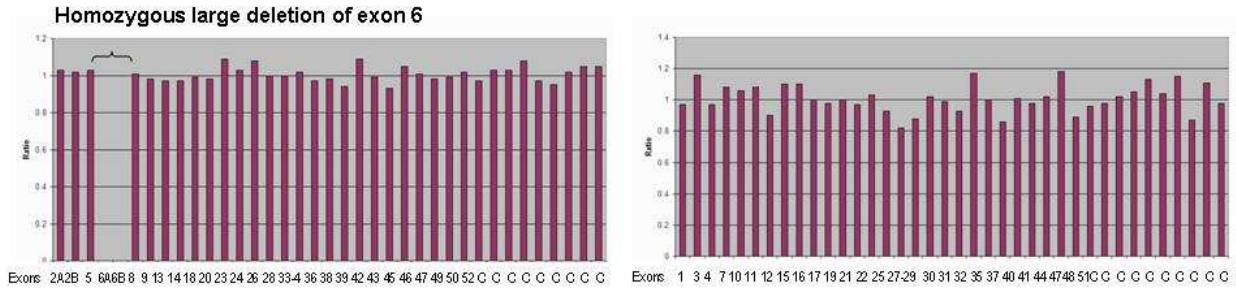

B. IP-2

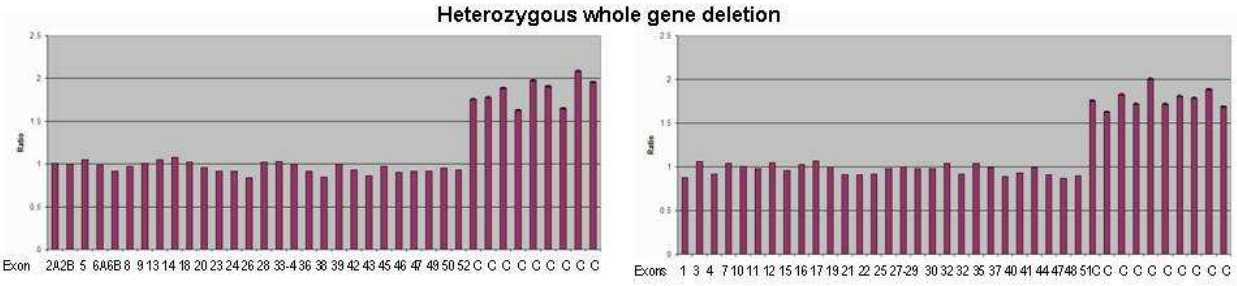

C. IP-3

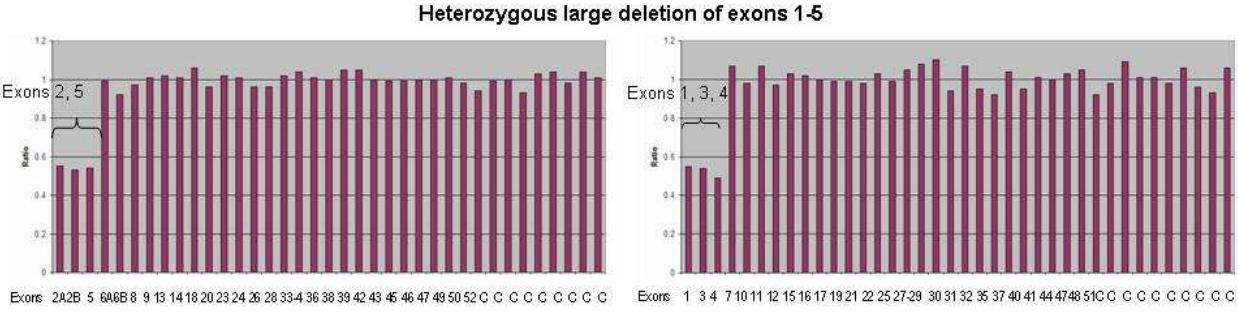

D. IP-4

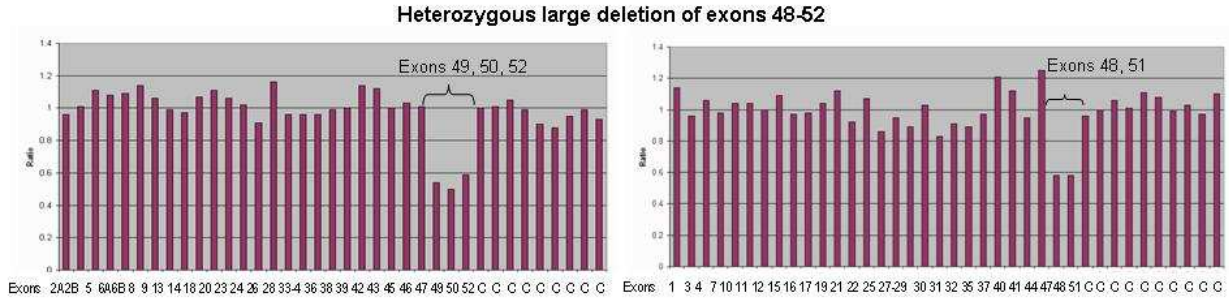

E. IP-5

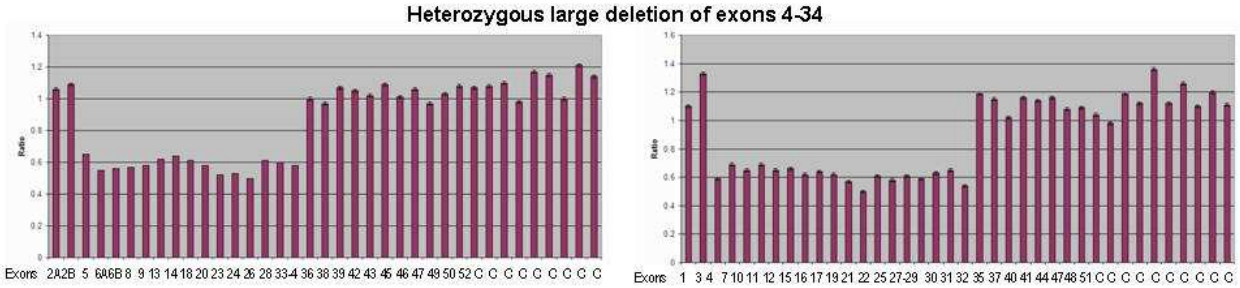

F. IP-6

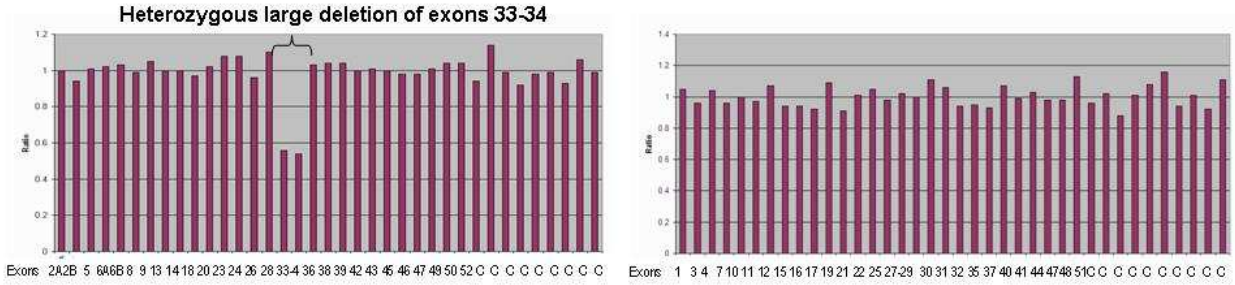

Figure 3.1 A-F. Multiple ligation-dependent probe amplification (MLPA) of 6 index patients (IPs). The X-axis represents the probes of each exon of *VWF* and control probes (C). Probes of 52 exons of *VWF* are divided in 2 different probemixes; Mix 1 (Left figures) and Mix 2 (right figures); there are two probes for the exons 2, 6, 28, 47. The heterozygous deleted exons are presented with half size of the peaks.

A heterozygous small deletion (p.Leu 757ValfsX22) together with a large deletion of exons 48-52 was detected in the IP-4 (Table 3.1, Figure 3.1D).

The IP-5 showed evidence of severe type 3 VWD. Numerous epistaxis, oral cavity bleedings, gastrointestinal bleedings and haematomas were reported by this patient. Laboratory data proved type 3 VWD (VWF:Ag <1%, VWF:RCo <6% and FVIII:C 2,4%). Surprisingly, the genetic investigation revealed only a heterozygous large deletion of exons 4-34 (Table 3.1, Figure 3.1E). Since this single defect could not explain the severe clinical picture, it could be speculated that another genetic alteration, affecting either structures outside the *VWF* or inside the *VWF* intronic region are involved. A second possibility is that two separate large deletions spanning together exons 4-34 affect both alleles without overlapping each other. Unfortunately, the parents were not available to prove this hypothesis.

An interesting case was IP-6 where we present combined VWD and haemophilia A (Figure 3.2a). The patient's laboratory data showed reduced VWF:Ag (17%), VWF:RCo (9%) and FVIII:C (1,9%). The genetic analyses of *F8* showed a missense mutation in exon 23, Asn2129Ser. This mutation is localized in the FVIII C1 domain and leads to impairment of FVIII binding to VWF.[96]

The mother was a carrier of the same gene defect although no bleeding history is reported in any family member from her site. The VWF:Ag and VWF:RCo were in the normal range. The patient's father displayed a significant decrease in VWF:Ag and VWF:RCo - 13% and 7%, respectively , FVIII: C of 18,5% and the VWF:RCo/ VWF:Ag ratio of 0,5 pointing out to type 2 VWD. The VWF multimer analyses depict a reduction of large multimers (located in the black box) typical for type 2A VWD (Figure 3.2b).

The sequencing of the *VWF* of the father of IP-6 showed no genetic alteration and MLPA revealed a large deletion of exons 33-34 (Figure 1.3F and Figure 3.2c).This genetic defect segregates in the family and was proven in 5 other members, including the IP-6 (Figure 3.2a). Clinically, the patient experienced bleedings in the oral cavity, ankle joint and haematomas. All bleeding events in the IP were presented with stronger severity compared to the one of his brother and father who did not bear the *F8* mutation but only the large deletion in *VWF*. The majority of mutations responsible for dominant type 2 VWD are missense

substitutions. Only one large deletion removing domains A1, A2 and A3 of VWF was previously reported in a patient with type 2A VWD.[97] Casari et al. showed in their study the mechanism of this dominant-negative large deletion that can cause severe type 2 VWD through *in vitro* coexpression of the wilde-type and the in-frame deleted VWF. They discovered that the altered VWF formed heterodimers and heterotetramers with wild-type VWF and these heterodimers act as terminators of the multimerization process in the Golgi compartment.[98]

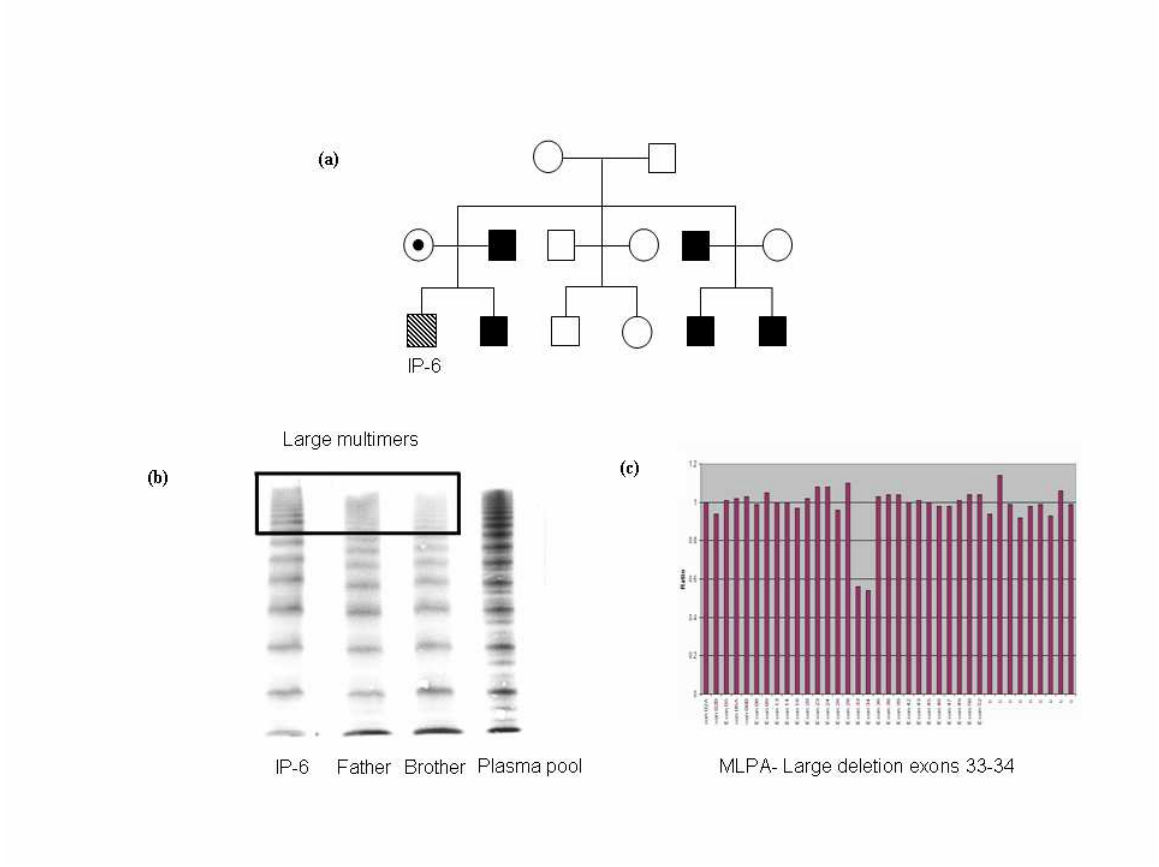

Figure 3.2
(a) Pedigree of a family with deletion of exons 33-34 of the VWF gene. **(b)** Results of multimer analysis of three family members that show reduction of large VWF multimers, marked with the black box, compared to pooled normal plasma. **(c)** MLPA of IP-6. The deleted exons 33 and 34 present with half size of the peaks.

■ = VWD affected male
□ = VWD unaffected male
○ = VWD unaffected female
◉ = haemophilia A carrier female
■ = combined VWD and haemophilia A male

No large deletion was detected in 11 index patients with type 1 VWD in whom VWF antigen level was more than 33 IU/dL. Previous studies have reported that VWF levels below the reference range but above 30IU/dL may often not be in linkage to the VWF locus.[42, 99]

In conclusion, our results indicate that large deletions should be taken into consideration for the diagnosis of type 3 VWD especially in patients without two clear causative mutations. The possibility of a large deletion should always be taken into consideration if sequencing results reveal the presence of homozygous polymorphisms or a homozygous mutation. Moreover, not only type 3 VWD patients but also patients diagnosed to have type 2 VWD in which no *VWF* mutation could be identified, should be analyzed for the presence of large deletions. Despite the fact that no large deletions were detected in patients with type 1 VWD in our study, we propose to investigate these patients for the presence of possible heterozygous large deletions when no causative mutations are identified. Finally, the MLPA assay is a rapid, simple and robust method for the routine diagnosis of large deletions.

Chapter 4

Insights into pathological mechanisms of missense mutations in C-terminal domains of von Willebrand factor causing qualitative or quantitative von Willebrand disease

Adapted from

Yadegari H., Driesen J., Pavlova A., Biswas A., Ivaskevicius V., Klamroth R., and Oldenburg J.,

Accepted to be published in Haematologica [In Press]

4.1 Abstract

The carboxy-terminal domains of VWF, D4-CK, are cysteine rich, implying their structural importance. The present study characterized the impact of five cysteine missense mutations residing in D4-CK domains on conformation and biosynthesis of VWF. These variants were identified as heterozygous in type 1 (p.Cys2619Tyr and p.Cys2676Phe), type 2A (p.Cys2085Tyr and p.Cys2327Trp) and as compound heterozygous in type 3 (p.Cys2283Arg) VWD. Transient expression of human cell lines with wild-type or mutant VWF constructs was performed. Quantitative and qualitative assessment of mutated recombinant VWF was done in comparison with recombinant wild-type VWF. Storage of VWF in pseudo-Weible-Palade bodies was studied with confocal microscopy. Structural impact of the mutations was analyzed by homology modeling. Homozygous expressions showed that these mutations caused defects in multimerization, elongation of pseudo-Weible-Palade and consequently secretion of VWF. Co-expressions of wild-type VWF and p.Cys2085Tyr, p.Cys2327Trp and p.Cys2283Arg demonstrated defect in multimer assembly, suggesting a new pathologic mechanism for dominant type 2A VWD due to mutations in D4 and B domains. Structural analysis revealed that mutations p.Cys2283Arg, p.Cys2619Tyr and p.Cys2676Phe disrupted intra-domain disulfide bonds, whereas p.Cys2327Trp might affect an inter-domain disulfide bond. The p.Cys2327Trp variant is distinguished from the other mutants by an electrophoretic mobility shift of the multimer bands. The results highlight the importance of cysteine residues within the C-terminal of VWF on structural conformation of protein and consequently multimerization, storage, and secretion of VWF.

4.2 Introduction

Types 1 and 3 VWD are characterized by quantitative deficiencies of VWF. This can resulte from relative (type 1) or absolute (type 3) deficiency in VWF production due to impaired synthesis, secretion, or half-life of the molecule.[3, 18, 100] The VWD type 2A, characterized by the absence of HMWM and decreased platelet-dependent function, is the most common form of VWD type 2.[51, 59] The loss of HMWM in type 2A VWD results from either mutations that impair assembly and secretion of VWF multimers or variants that increased susceptibility to proteolytic cleavage by ADAMTS13. [9, 101, 102]

The pre-pro-VWF precursor comprises of a signal peptide and repeated domains arranged in the order D1-D2-D′-D3-A1-A2-A3-D4-B1-B2-B3-C1-C2-CK. In the ER, pro-VWF assembles into dimers through disulfide bonds between CK domains, and is then transported to the TGN. There the dimers assemble into multimers by N-terminal disulfide bonds aligned with formation of helical tubules in nascent WPB.[27, 32] The domains may be characterized as functional or structural, depending on whether they have specific functions in haemostasis or in forming ultralong concatamers. Although carboxy-terminal (C-terminal) of VWF, including D4, B and C domains, is a cysteine-rich area, which may imply structural importance, no particular function for most of these domains is assigned.[16] Recently, the classical annotation of the C-terminal domain has been updated by Zhou *et al.*, where the previous B and C regions of VWF are re-annotated as 6 tandem von Willebrand C (VWC) and VWC-like domains, C1-C6.[19] Additionally, it has been demonstrated that the VWF C-terminals zip up and form a structure resembling a bouquet of flowers, where the A2, A3, and D4 domains comprise the flowers part and the six VWC domains configure the stem.[19, 31]

In this study we analyzed five different VWF mutations, affecting cysteine amino acids in the D4, B, C2 and N- terminal of CK domains, four of which have been previously reported in our work.[103] Interestingly, these gene alterations were associated with either quantitative (types 1 and 3) or qualitative VWD (type 2A). The mutations have been transiently expressed *in vitro,* and their effect on the multimer assembly, biogenesis of WPB and secretion has been characterized. Possible structural impact of these cysteine mutations was additionally studied

by homology modeling. The results of the present study expand our understanding of the pathophysiological mechanisms of C-terminal domains VWF mutations which will help in establishment of phenotype-genotype correlations.

4.3 Materials and Methods

4.3.1 Patients

Five patients, diagnosed with VWD (2 patients with type 1, 2 patients with type 2A and 1 with type 3) were included in the study. Bleeding severity was quantified by the bleeding score (BS) calculated on the basis of condensed MCMDM -1 VWD questionnaire.[104] This study was approved by the local ethics committee and informed consent was obtained from all patients (vote 091/09).

Coagulation and multimer analysis

Laboratory investigation of VWF antigen (VWF:Ag), VWF ristocetin cofactor activity (VWF:RCo), FVIII coagulant activity (FVIII:C) and VWF multimers (1.2% [w/v] and 1,6% [w/v] agarose gels) was performed.[60, 103] VWF multimer profiles were classified as normal or abnormal.

Mutation detection

All mutations were identified by direct sequencing of *VWF* coding region, exon–intron boundaries and 5’ and 3’ non-coding regions.[103]

4.3.2 Expression studies

Plasmid constructs

Plasmid pMT2-VWF containing the human full-length wild-type (WT) VWF cDNA was kindly provided by Professor Schneppenheim (Department of

Pediatric Hematology and Oncology, University Medical Center Hamburg-Eppendorf, Hamburg, Germany). The mutant constructs were generated using a QuickChange II XL site-directed mutagenesis kit (Stratagene, La Jolla, CA, USA). The sequences of all constructs were verified by DNA sequencing.

Cell culture and transfection

Human embryonic kidney cell lines (HEK 293T; DSMZ, Braunschweig, Germany) were used to evaluate the secretion and intracellular retention of WT and mutants recombinant VWF (rVWF). HEK293 cell lines (DSMZ, Braunschweig, Germany) were used to analyze the intracellular location of VWF by confocal immunofluorescence microscopy. Both cell lines were cultured in Dulbecco's modified Eagel medium (DMEM) containing 4.5g L^{-1} glucose and 2mM L-glutamine supplemented with 10% (v/v) fetal bovine serum, 100IU mL^{-1} penicillin, 100 µg mL^{-1} streptomycin and 0.25 UG/ML Fungizone (all reagents supplied by Life Technologies, CA, USA) at 37℃ in 5% CO2 atmosphere.
Cells were transiently transfected with 8µg of WT-VWF or mutated VWF constructs using liposomal transfer (Lipofectamine 2000; Life Technologies, CA, USA) according to the manufacturer's instructions. Co-transfections were performed using an equal amount of WT and mutant vectors (4 µg each of WT and mutant DNA) to reproduce the patients' heterozygous state. Seventy-two hours after transfection of HEK293T cells, supernatants were collected and cells were lysed for analysis of intracellular VWF. VWF secreted in the medium was concentrated on Amicon Centrifugal 50K filter devices (Millipore, USA) to one-forth of the original volume before subsequent analysis. The transfected cells were lysed by 3 rounds of freezing (-80˚C) and thawing in lysis buffer (0.1M Tris/HCl pH 8.0; 0.6 [v/v] Triton X-100).[105]

4.3.3 Quantitative and qualitative analysis of rVWF

The amount of VWF:Ag secreted into the medium and VWF:Ag present in the cellular lysate were determined, and the values were expressed as a percentage of the corresponding WT recombinant VWF. Activity of secreted

rVWF was assessed by binding to platelet GPIb, collagen type III (VWF:CB), and VWF:RCo. The VWF activities were expressed as ratios to secreted VWF. VWF:GPIb binding was determined using a particle enhanced assay (Siemens Healthcare, Marburg, Germany) and VWF:CB was assessed by ELISA method (Technoclone, Vienna, Austria) according to the manufacturer's instructions. Comparison between the mean values of the groups was performed with the Student *t*-test. Multimer analysis of concentrated secreted rVWF was performed as described above.

4.3.4 ADAMTS13 assay

To assess the susceptibility of mutants of VWF to proteolysis, full-length WT and mutated rVWF (6μg/ml) were cleaved by 3μg/ml of recombinant ADAMTS13 (R&D systems, USA) in the presence of 1.5M urea at 37˚ C for 2 hours following the manufacturer's instructions. The multimer patterns of mutated and rVWF-WT were visually compared on agarose gel electrophoresis after ADAMTS13 digestion.

4.3.5 Immunofluorescence analysis

HEK293 cells were grown on gelatin pre-coated glass coverslips in 24-well plates. Cells were fixed 48 hr after transfection by 4% (w/v) paraformaldehyde in PBS, blocked with 0.1% (v/v) Triton-X 100 in PBS azide supplemented with 10% (v/v) FBS. Cells were incubated with first antibodies for 2 hr and then with fluorescence-conjugated secondary antibodies for 1 hr. Polyclonal sheep to human VWF (abcam, England) and rabbit anti–human VWF antibodies (Dako, Glostrup, Denmark) were used to visualize VWF. Monoclonal anti-GM130 (BD Bioscience, CA) and polyclonal rabbit anti-human TGN46 (Sigma-Aldrich, USA) were used to stain *cis*- and *trans*-Golgi networks, respectively.[106] To visualize the endoplasmic reticulum (ER), the HEK293 cells were prepared and stained with rabbit anti-human protein-disulfide isomerase (PDI) antibody using SelectFX® Endoplasmic Reticulum Labeling kit (Life Technologies, CA, USA) according to the manufacturer's instructions. Secondary antibodies were

conjugated with either AlexaFluor-488 or AlexaFluor-594 (Life Technologies, CA, USA). The coverslips were mounted onto microscope slides with Vectorshield (Vector Labs, Burlingame, CA, USA) and analyzed with the Olympus Fluo View FV1000 or Leica SL confocal microscope.

4.3.6 Structure analysis

Homology modeling of VWF C1, C5, C6 domains

Homology models for the C1, C5, and C6 domains were constructed using various software packages. The domain boundaries for C1, C5, and C6 domains were based on domain annotations from a recently published article.[19] The sequences for the respective domains were from the VWF (Accession number P04275) full length sequence. Templates for each of the domains were searched on the LOMETS server from Zhang.[107] Close packed alignments (using the conserved cysteines as guideposts) were generated between the best LOMETS templates and the original domain sequences using Jalview. The alignments as well as the templates were entered into YASARA version 12.8.6[108] to generate full-length models. The resulting models were further refined by a 500ps MD simulation (AMBER03 force field) in YASARA version 12.8.6. The models with the lowest force field energies were chosen as the final models for the respective domains. The stereochemical quality of these models were checked on the MOLPROBITY server [http://molprobity.biochem.duke.edu/;accessed between 15.07.2012 and 15.09.2012].[109] The monomer models were run on the online server CLUSPRO in dimer mode (http://cluspro.bu.edu/home.php;accessed between 15.08.2012 and 15.10.2012) and the best dimers were chosen based on cluster size for further interface analysis.[110] Impact of mutation on folding was calculated using the FOLDX plugin incorporated in YASARA version 12.8.6.[111]

Molecular models of the VWF mutations

The missense mutations were modeled on the final refined wild-type VWF domain structures. The mutant structure was optimized for the best possible rotamer using the SCRWL library in YASARA version 12.8.6.[112] The variant structures were subjected to rounds of steepest descent and annealing energy minimizations. Subsequently MD simulation was performed for 10 ns (nanosecond) for each mutated structure as well as the wild type. The simulation trajectory for both wild type and mutant proteins were analyzed with respect to each other.

4.4 Results

4.4.1 Characterization of patients

Genotype, laboratory parameters, bleeding symptoms and bleeding scores (BS) of all five patients are presented in Table 4.1. Mutation analysis revealed 6 different variants (p.Cys1227Arg, p.Cys2085Tyr, p.Cys2283Arg, p.Cys2327Trp, p.Cys2619Tyr, p.Cys2676Phe) all presented in heterozygous state. In four patients the mutations were detected as single gene defect associated with type 2A VWD (patients 1 and 3) and type 1 VWD (patients 4 and 5). Both mutations p.Cys2283Arg and p.Cys1227Arg were detected in type 3 VWD (patient 2). All mutations, except p.Cys1227Arg were localized in the C-terminal end of VWF (domain D4, B, C2 and C2-CK, corresponding to D4, C1, C5 and C6 domains up-dated by Zhou *et al*).[19] Bleeding symptoms and BS were recorded in relation to the VWD type.

#	VWD Type	Nucleotide exchange	AA exchange	Domain original designations	Domain updated designations	VWF:Ag IU/dL	VWF:RCo IU/dL	FVIII:C IU/dL	Multimer pattern	Bleeding Score (BS)	Bleeding symptoms
1	2A	c.6254G>A	p.Cys2085Tyr	D4	D4	22	13	42	Abnormal	13	1,2, 3, 5
2	3	c.6847T>C	p.Cys2283Arg	D4	C1	3	5	6	No multimer	15	1, 2, 3, 5, 6, 10
		c.3679T>C	p.Cys1227Arg	D3							
3	2A	c.6981T>G	p.Cys2327Trp	B	C1	13	7	22	Abnormal	20	1, 2, 3, 4, 6, 8, 9
4	1	c.7856G>A	p.Cys2619r	C2	C5	37	43		Normal	6	5, 7
5	1	c.8027G>T	p.Cys2676Phe	C2-CK	C6	39	30	84	Normal	3	1,7

Table 4.1. Mutations and phenotypic characteristics of patients.
The numbers listed in bleeding symptoms column represent: 1 = Epistaxis, 2 = easy bruising, 3 = bleeding from minor wounds, 4 = bleeding from oral cavity, 5 = bleeding after tooth extraction, 6 = postoperative bleeding, 7 = menorrhagia, 8 = postpartum hemorrhage, 9 = muscle hematomas, 10 = CNS bleeding.

4.4.2 Expression of VWF mutations in human cell lines

To characterize the effect of the identified mutations on VWF processing, transient transfections were performed and rVWF:Ag levels were measured in both the conditioned culture media and cell lysates and expressed as a percentage of the corresponding wild-type rVWF levels. Five expression vectors corresponding to each mutation were homozygously expressed in HEK293T cells. All mutants demonstrated severely impaired secretion. The detected rVWF:Ag levels in medium were significantly lower compared to the WT, ranging from 7% to 23% of rVWF-WT (Figure 4.1, left side). To mimic the heterozygous patient state, co-expression of four mutants (p.Cys2085Tyr, p.Cys2327Trp, p.Cys2619Tyr, p.Cys2676Phe) together with WT were additionally performed. The rVWF:Ag values showed reduction in secretion, in the range of 45.7 to 59.5% of WT (Figure 4.1, right side).

Furthermore, co-expression of variants p.Cys2283Arg and p.Cys1227Arg (representing the compound heterozygous state of type 3 VWD patient) resulted in strongly reduced secretion of VWF to 19% (Figure 4.1, right side).

The measurement of intracellular rVWF:Ag of all mutants showed values higher than that of the WT, indicating intracellular retention of rVWF-mutants (Figure 4.1).

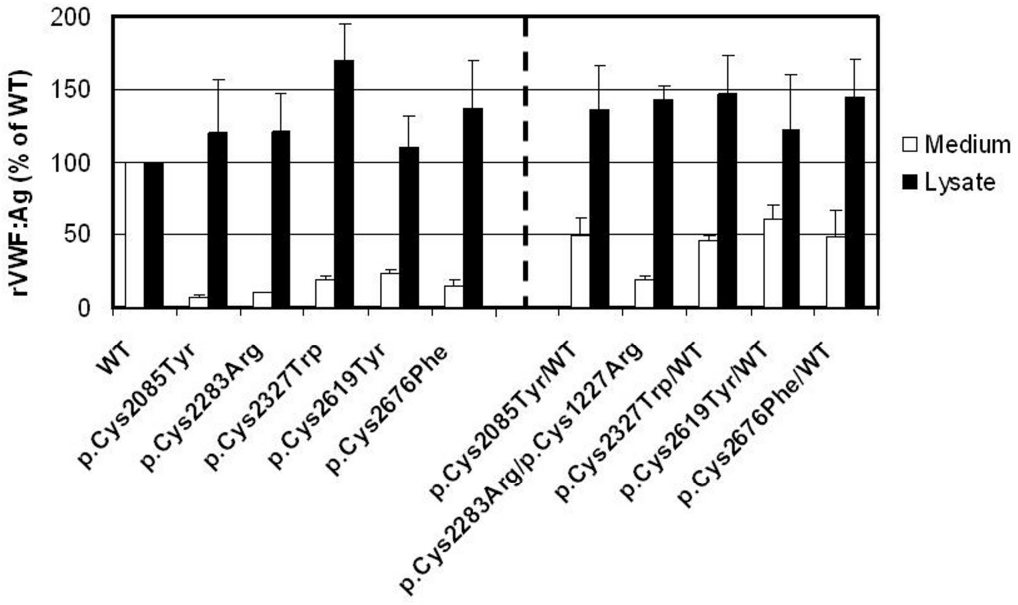

Figure 4.1. Recombinant VWF levels in medium and lysates.
Recombinant VWF antigen levels (VWF:Ag) in medium (white bars) and lysate (black bars) are expressed as percentage relative to the amount of VWF:Ag in the medium and lysate of cells expressing WT-VWF. Each column represents the mean and standard deviations of at least three independent experiments in triplicate. Co-transfections of WT and mutant VWF cDNA were done with a 1:1 ratio.

4.4.3 Functional characterization of recombinant VWF mutants

The multimer distribution of the recombinant variants demonstrated a range of structural abnormalities (Figure 4.2). Single transfections rVWF-p.Cys2085Tyr, p.Cys2283Arg and p.Cys2676Phe exhibited only dimers and tetramers. Multimer analysis of secreted rVWF-p.Cys2327Trp revealed a complete lack of intermediate and high molecular weight multimers, whereas rVWF-p.Cys2619Tyr showed loss of most of intermediate multimers and lack of HMWM (Figure 4.2 A). Interestingly, variant C2327W additionally showed shift in mobility of multimer bands (Figure 4.2 A).

Figure 4.2B illustrates the multimer patterns for co-expressed mutants and WT as well as for co-expression of the two mutants p.Cys2283Arg and p.Cys1227Arg, identified in the type 3 VWD patient. The co-expression of WT with mutants p.Cys2619Tyr and p.Cys2676Phe led to secretion of the full range

of VWF multimers. This profile corresponds to the multimer pattern observed in patient with type 1 VWD (Figure 4.2C). The multimer structure of the second group of co-expressions of p.Cys2085Tyr/WT, p.Cys2327Trp/WT and p.Cys2283Arg/WT showed a reduction of the largest multimers in secreted VWF compared with WT which is in correlation with type 2A patients' phenotype. The observed reduction is so intensive in co-expressions of p.Cys2085Tyr/WT that even leads to the loss of the largest multimers. The p.Cys2283Arg/p.Cys1227Arg co-expression resulted in detection of only a few low molecular weight multimers.

Functional assessment of heterozygously expressed variants are presented as ratios of VWF:RCo, GPIb binding and VWF:CB to VWF:Ag of secreted VWF in Table 4.2. Since the VWF levels in media of single mutant transfection of mutants were too low for reliable quantification, VWF activity assays were only performed for co-expressions of mutant/WT. Co-expressions p.Cys2085Tyr/WT, p.Cys2283Arg/WT and p.Cys2327Trp/WT with impaired multimer structure showed decrease in ratios VWF:RCo, GPIb binding and CB to VWF:Ag compared with those of rVWF-WT ($p<0.05$), while variant p.Cys2619Tyr/WT with a normal multimer had normal binding activities as expected. However, p.Cys2676Phe/WT revealed reduced VWF activities ($p<0.05$ vs. wild type) in spite of normal multimer.

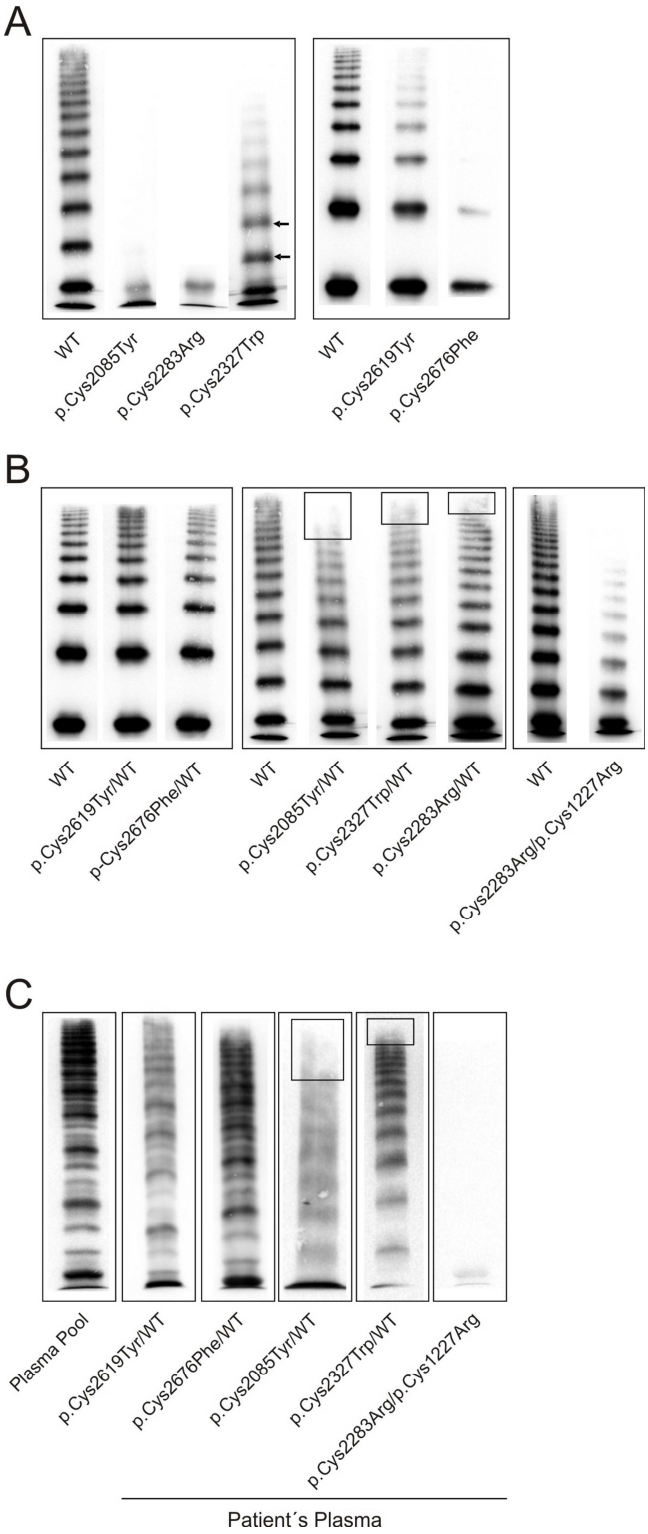

Figure 4.2. VWF multimeric analysis of patients and secreted rVWF after SDS-agarose gel electrophoresis. **Panels A and B** illustrate multimer analysis of rVWF-mutants in medium after single transfections and cotransfections, respectively, compared to rVWF-WT. Arrows indicate anodic shifts of multimeric bands observed for rVWF-p.Cys2327Trp. Boxes indicate reduction or loss of large multimers. **Panel C** represents multimer analysis of patients' plasma.

	VWF:RCo/VWF:Ag	VWF:GPIb/VWF:Ag	VWF:CB/VWF:Ag
WT	**0.779 ± 0.205**	**0.717± 0.108**	**0.625 ± 0.103**
p.Cys2085Tyr/WT	0.632 ± 0.131	0.538 ± 0.036	0.408 ± 0.139
p.Cys2283Arg/WT	0.496 ± 0.129	0.581 ± 0.068	0.543 ± 0.131
p.Cys2327Trp/WT	0.465 ± 0.026	0.591 ± 0.064	0.471 ± 0.017
p.Cys2619Tyr/WT	0.703 ± 0.133	0.709 ± 0.054	0.526 ± 0.063
p.Cys2676Phe/WT	0.611± 0.057	0.529 ± 0.035	0.426 ± 0.088

Table 4.2. Functional assays of secreted recombinant VWF proteins.
Mean and standard deviations of ratios VWF:RCo, GPIb and CB to VWF:Ag of three independent co-experiments in triplicate.

4.4.4 Susceptibility of variants to cleavage by ADAMTS13

We investigated whether mutants have altered susceptibility to ADAMTS13 proteolysis. Proteolytic degradation of rVWF-mutants was compared to that of the rVWF-WT. No difference in the sensitivity of the rVWF mutants to cleavage by ADAMTS13 has been demonstrated (Figure 4.3).

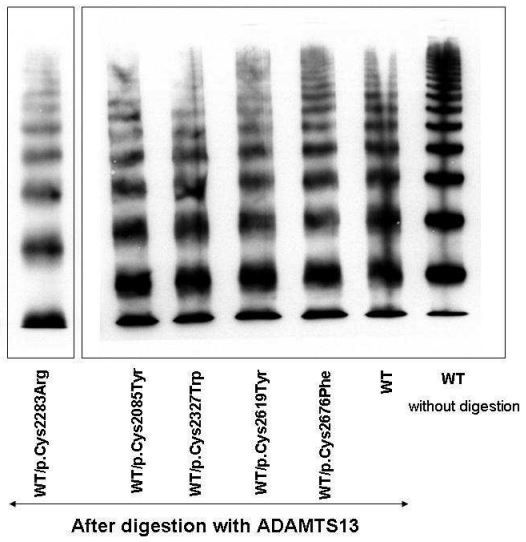

Figure 4.3. Multimer analysis of heterozygously expressed rVWF after digestion with rADAMTS13 *in vitro*. The secreted rVWF was concentrated and then was cleaved by recombinant ADAMTS13. The figure illustrates the multimer pattern of digested mutated and rVWF-WT after electrophoresis on 1.6% SDS_agarose gel.

4.4.5 Intracellular localization

Intracellular trafficking and the impact of mutations on granule formation were analyzed after expression of mutants in HEK293 cells. HEK293 cells form pseudo-WPB granules when transfected with rVWF-WT.[101, 113] Confocal microscopy showed no retention of all mutant rVWF in either the ER or in the cis- or trans-Golgi compartments (Figures 4.4 and 4.5). Each of the VWF mutants was able to form pseudo-WPB storage granules (Figure 4.6, presented as small dots), although those granules had different morphology from normal cigar-shaped granules formed by rVWF-WT. The majority of the pseudo-WPB granules formed by mutants were relatively shorter. We also investigated the impact of VWF variant heterozygosity on storage in pseudo-WPB granules. Upon co-transfection with rVWF-WT, the defects in the elongation of the pseudo-WPB granules caused by mutations were partially corrected.

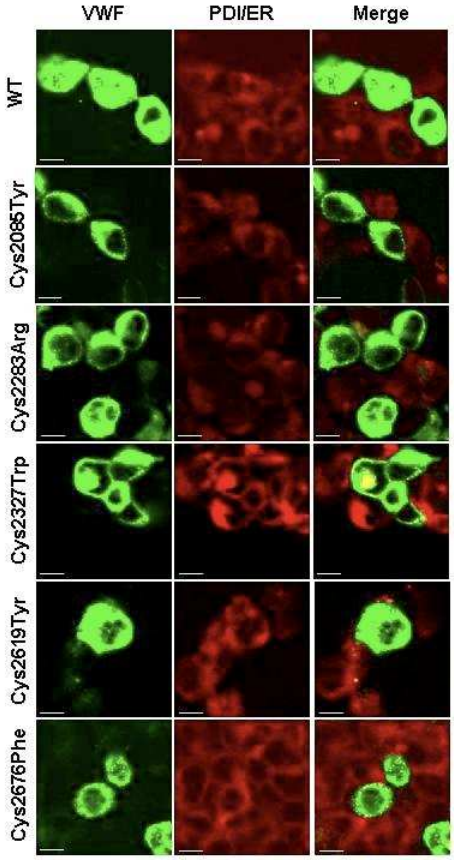

Figure 4.4 Subcellular localization of rVWF-WT and variants in relation to endoplasmic reticulum (ER) in transfected HEK293 cell lines.
Fixed cells were stained for VWF (green channel, left panel) and for PDI (ER marker, red channel, middle panel). Right panel illustrates the merge of green and red channels. Scale bars, 10 µl.

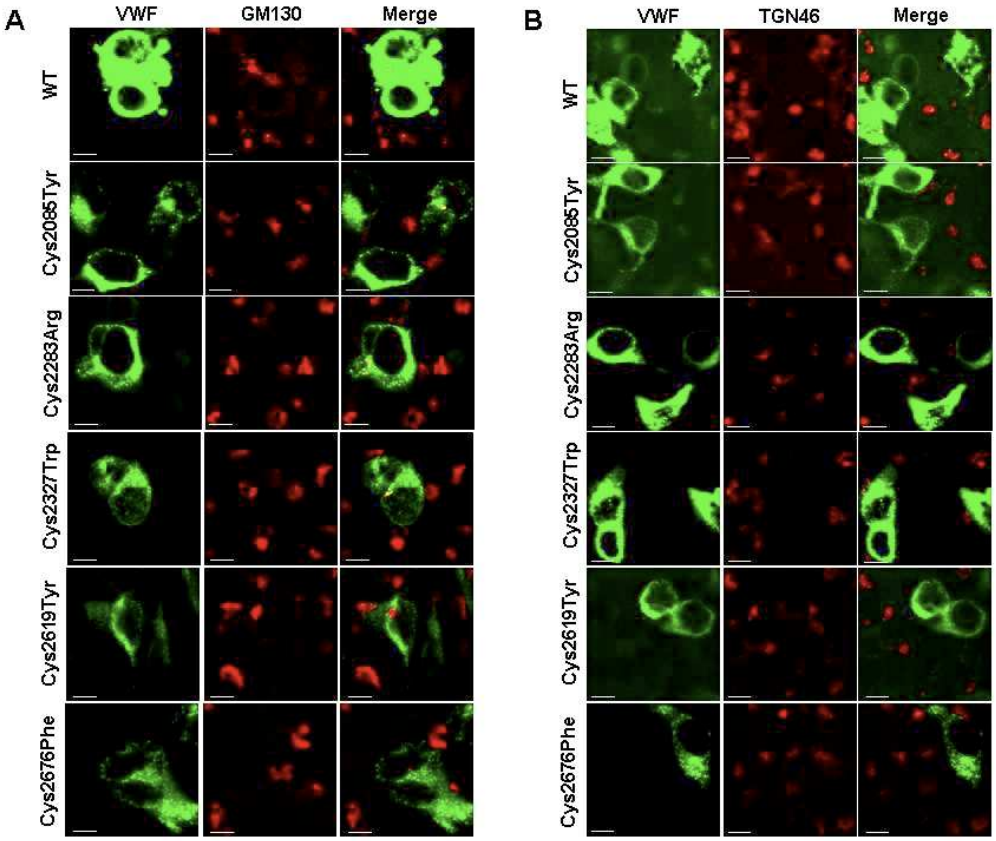

Figure 4.5. Subcellular localization of rVWF-WT and variants in transfected HEK293 cell lines.
In Panel A, fixed cells were stained for VWF (green channel, left panel) and for GM130 (Cis-Golgi marker, red channel, middle panel). Right panel illustrates the merge of green and red channels.
In Panel B, fixed cells were stained for VWF (green channel, left panel) and for TGN46 (Trans-Golgi marker, red channel, middle panel). Right panel illustrates the merge of green and red channels. Scale bars, 10 µl.

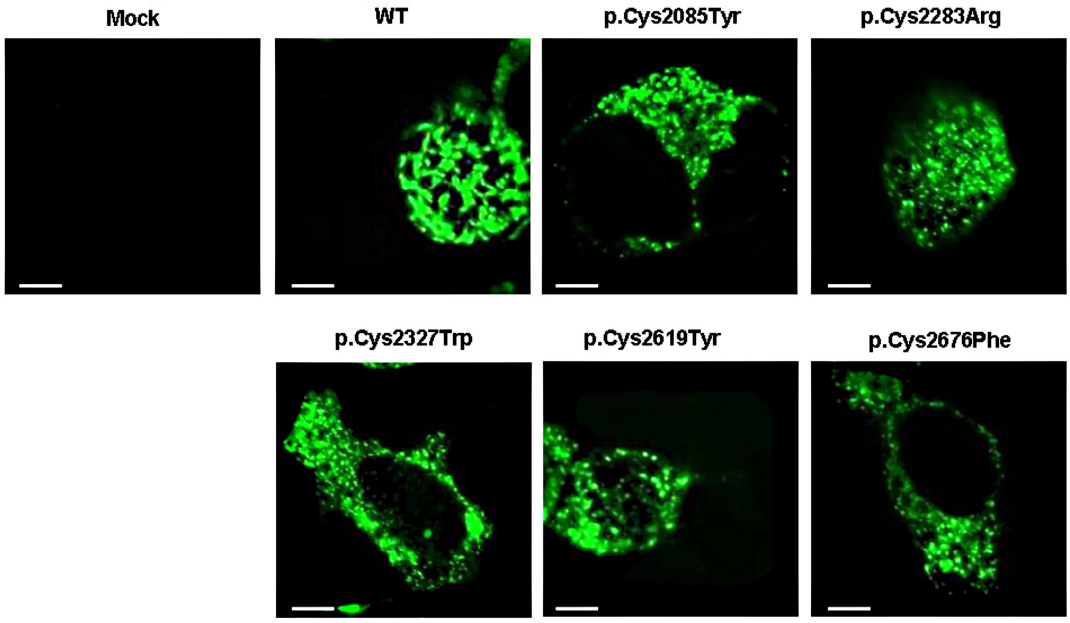

Figure 4.6. Intracellular storage of rVWF-WT and mutants in HEK293 cells.
The pseudo-WPB granules formed after single transfections of HEK293T cells with WT and mutated constructs and mock transfected cells. Pseudo-WPB granules are shown in green (VWF staining). Pseudo-WPB granules in cells expressing rVWF-WT have cigar-shaped appearance, while they are round and shorter in cells expressing rVWF-mutants. Scale bar = 10μm.

4.4.6 Impact of the mutations on VWF structure

Homology modeling

The C1, C5 and C6 domains (according to the Zhou *et al*) are cysteine rich domains characterized by multiple cysteine disulfide bonds.[19] The domains comprise of short beta strands linked by a combination of beta turns and hairpins with the occasional short beta bulge (C6) or alpha helix (C5 & C6) (Figure 4.7). Only the C1 domain shows unpaired cysteines (n=4) (Figure 4.7), the remaining cysteines form intra-domain/intrachain disulfide bonds.

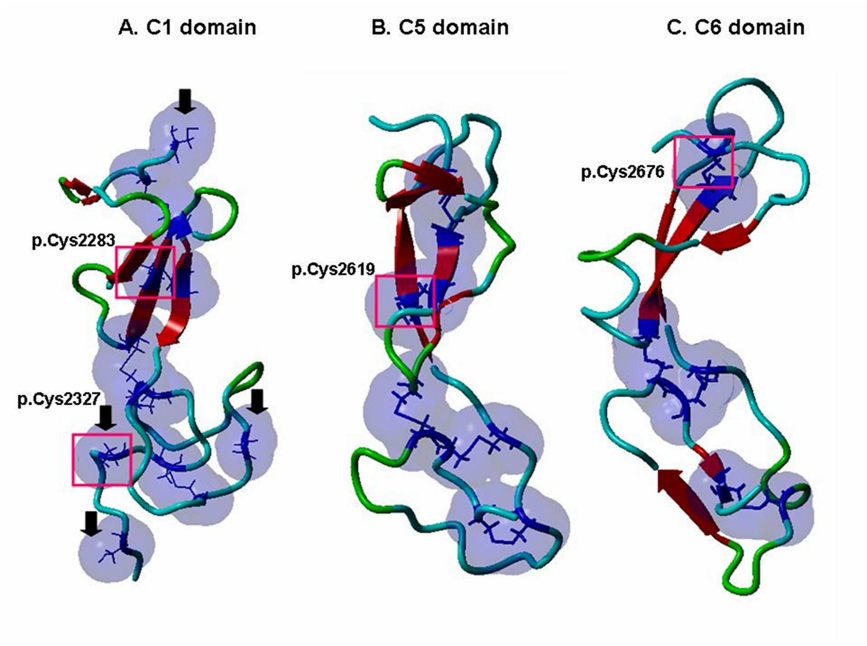

Figure 4.7. Homology models for C1, C5 and C6 domains.
Panels A, B and C show ribbon diagrams for the homology models of C1, C5 and C6 domains. The cysteines (unpaired and bound) are represented in stick forms. The accessible surface areas of the unpaired and bound cysteines are represented as blue spheres. The arrows in Panel A show the unpaired cysteines in Domain C1. The pink boxes show the position of Cys2283 and Cys2327 in C1 domain, Cys2619 in C5 domain and Cys2676 in C6 domain.

MD simulation and stability prediction

The simulation of the monomeric C1, C5 and C6 domains showed high RMSD (root mean square deviation) which finally stabilized between 2-2.5A°. Comparison of trajectory RMSD for the short period of 10 nanoseconds showed differences between the mutation and the wild type structures (Table 4.3). Trajectory analysis for other components such as accessible surface area and the radius of gyration also showed differences between the mutations and the wild type (Table 4.3). Folding energy calculations showed a high impact for all the mutations except p.Cys2327Trp in C1 domain. The p.Cys2283Arg mutation results in the replacement of a buried conserved disulfide bonded cysteine residue to a polar, charged and large Arg residue which is partly surface exposed (Figure 4.8, Panel A). The p.Cys2327 residue was the only cysteine that is observed at the interface of the C-domain dimer models (models not shown). The p.Cys2327Trp mutation was also the only cysteine residue

mutation amongst the ones we reported which belongs to the unpaired cysteine (no intra-domain disulfide bond) category. This cysteine was partly surface exposed and also present at the C1-C1 dimer interface (in the dimer model) (Figure 4.8, Panel Biii) at the C-terminal end of the domain (which connects to the C2 domain). The affected cysteine in the C5 domain p.Cys2619Tyr represents the substitution of a conserved disulfide bonded cysteine with an aromatic tyrosine side chain. The disulfide bond for the p.Cys2619 residue belongs to the RHStaple category of disulfide bonds (Table 4.4). The mutation p.Cys2676Phe in the C6 domain results in the replacement of a highly conserved disulfide bonded cysteine with a large aromatic and highly hydophobic Phe side chain. During simulation the mutated Phe side chain is accommodated within the domain (Figure 4.8, Panel D).

Residue	B (Disulphide Bond)	A.S.A	R.O.G	R.M.S.D	Charge	ΔΔG
p.Cys2283Arg	4CYS-30CYS	2.01/47.02	17.42/20.03	2.24/4.67	+	+12.20
p.Cys2327Trp	-	47.25/83.91	17.42/18.01	2.24/2.32	0	+0.17
p.Cys2619Tyr	26CYS-42CYS	44.40/139.98	16.32/18.15	2.13/3.24	0	+7.65
p.Cys2676Phe	3CYS-30CYS	1.07/3.79	17.58/16.46	2.07/3.52	0	+8.51

Table 4.3. Structural changes observed during MD.
The structural characteristics are represented side by side for wild type/mutant residue. B: Bonds broken/added post mutation, A.S.A: Average surface accessible area for the simulation trajectory (in Angstrom units), R.O.G: Radius of gyration for the simulation trajectory (in Angstrom units), R.M.S.D: Average R.M.S.D for the simulation trajectory (in Angstrom units), Charge: Charge added or removed on mutation, ΔΔG: Average change in folding energy for mutation calculated with FOLDX [The stability of the mutated structure was estimated as the difference between the free energy (calculated from folding/unfolding algorithms) of the wild type protein and that of the mutant protein represented as ΔΔG values (stability/free energy changes);reported in kJ/mol; higher values indicate an unstable protein]. The numbering of cysteines mentioned in the second column is according to their linear appearance in the modelled domain structures.

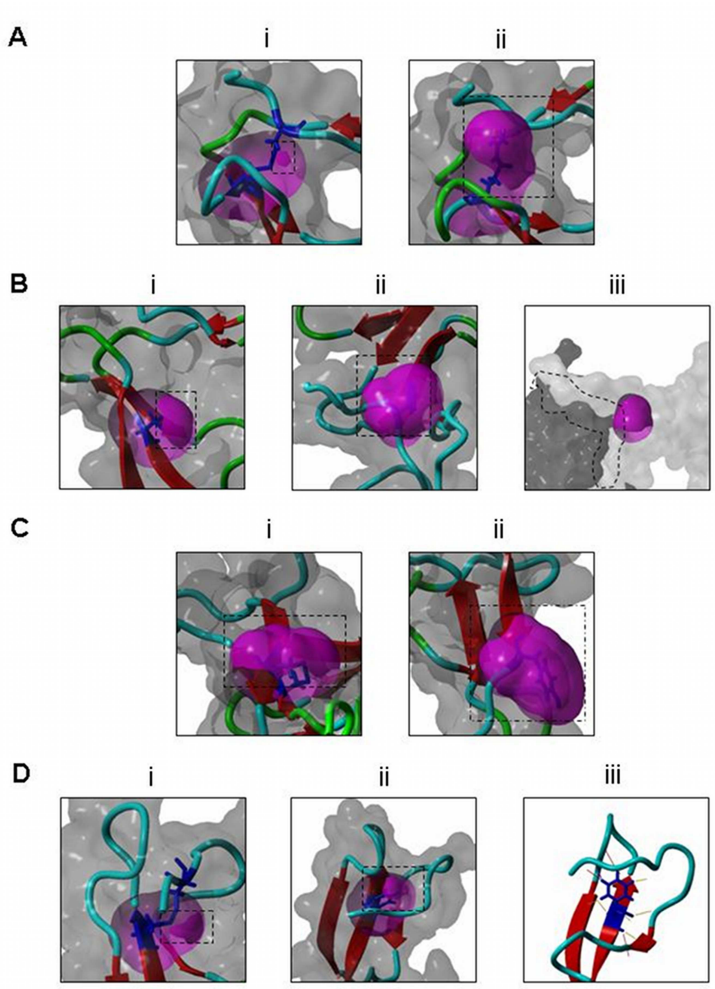

Figure 4.8. Close-up view of mutated and wild type residue after MD simulation. The representations are in surface diagrams with the backbone depicted in ribbon form. The affected residues are illustrated as blue stick representations. The surfaces of the model and affected residue are depicted in gray and magenta surface representations. The accessible surface area for the residues is highlighted by dotted rectangles and squares.
Panel A shows the wild type p.Cys2283 (i) and mutant p.Cys2283Arg (ii) after 10 nanoseconds of MD simulation. The cleavage of a disulfide bond and a distinct gain in accessible surface area is noticeable for the mutant residue. **Panel B** shows the wild type p.Cys2327 (i), mutant p.Cys2327Trp (ii) and the C1 dimer interface (Iii) after 10 nanoseconds of MD simulation. The Figure (iii) emphasizes the closeness of this locus to the hypothetical interface area (the neighboring surfaces of the individual monomers are colored in separate shades of gray and the interface is marked by dotted lines). The mutant residue shows a gain in accessible surface area with most of the Trp aromatic side chain exposed to the surface. **Panel C** shows the wild type p.Cys2619 (i) and mutant p.Cys2619Tyr (ii) in C2 domain after 10 ns of MD simulation. The mutant residue shows the breakage of disulfide bond and a large aromatic Tyr side chain almost completely surface exposed. **Panel D** shows the wild type p.Cys2676 in C6 domain (i), mutant p.Cys2676Phe (ii) and contact interference (iii) after 10 nanoseconds of MD simulation. The Fig (iii) shows mutated Phe residue accommodated into the protein scaffold resulting in contact problems with the neighbouring residues which are shown as colored lines.

Domain	Disulfide bond	Chi1	Chi2	Chi3	Chi2´	Chi1´	Type of Disulfide bond
C1	4 CYS-30CYS	-165.6	79.7	77.3	130.3	-143.8	-RHSpiral
C5	26CYS-42CYS	-43.5	-101.8	91.3	-86.9	-50.5	-RHStaple
C6	3CYS-30CYS	-66.8	-169.6	-101.3	169.0	59.5	+/-LHHook

Table 4.4. Cysteine Disulfide bonds.
The table lists the torsional angles for disulfide bonds on which mutations have been identified and the classification of these disulfide bonds based on the nature of (+or-) the torsional angles. Classification based on the sign of disulfide bonds (+: grey,-: blank) is annotated from previous literature as well as disulfide bond analysis file (disulfide_analysis_06_Aug_2012.zip) accessed on 07/10/2012 (http://www.med.unsw.edu.au/CRCWeb.nsf/page/Disulfide+Bond+Analysis).

4.5 Discussion

This study presents the functional characterization of five cysteine mutations occurring in the C-terminal domains of VWF. The results showed that these mutations had disruptive impacts on multimerization, storage and consequently secretion of VWF. The last two characteristics were partly corrected when the mutations were co-expressed with rVWF-WT. While the multimer structures of p.Cys2676Phe and p.Cys2619Tyr were completely corrected by co-expression with rVWF-WT, co-expressions of rVWF-WT and p.Cys2085Tyr, p.Cys2327Trp and p.Cys2283Arg showed loss or reduction of large multimers indicating a dominant negative effect of these mutations on multimerization. In agreement with our finding, previous studies have reported impaired multimerization and intracellular retention of VWF for some homozygously expressed cysteine missense mutations at the C-terminal of VWF.[86, 114, 115] Nevertheless, this study demonstrates for the first time defect in multimer assembly by heterozygous mutations occurring in the D4 and B domains, and presents a new pathologic mechanism for dominant type 2A VWD.

All mutants exhibited apparent intracellular retention. However, when the total produced amount of rVWF (sum of VWF:Ag in medium and lysate) was calculated, all mutant rVWF constructs (except p.Cys2327Trp) demonstrated statistically significant reduced expression of rVWF compared to rVWF-WT

($p<0.05$). These data suggest that the investigated mutations might additionally lead to increased intracellular degradation or decreased synthesis. The confocal microscopy results excluded retention of mutant rVWFs in the ER and cis- and/or trans-Golgi compartments. Punctuate granular pattern observed in immunofluorescent staining showed that the mutations interfere with the normal elongation of pseudo-WPBs. Previous investigations reported impaired formation of normal elongated pseudo-WPB granules for *in vitro* expression of variants located in propeptide, D3 and C-terminal VWF domains. [106, 115, 116]

Co-expressions of WT and either p.Cys2085Tyr, p.Cys2327Trp, p.Cys2619Tyr or p.Cys2676Phe mutans clearly reproduced the phenotype observed in heterozygous patients. Co-expression of p.Cys2283Arg and p.Cys1227Arg variants caused strong reduction in secretion of rVWF, suggesting that these mutations are causative for low VWF antigen in patient's plasma. It is already known that p.Cys1227 in the D3 domain participates in an intersubunit disulfide bond, critical for multimerization.[117] Our *in vitro* experiments clearly demonstrated that the p.Cys2283Arg variant also leads to defect in multimeristion assembly in both homozygous and heterozygous states. However, the VWF antigen levels and multimer analysis of the co-expressed mutants and patient's plasma showed slight discrepancies. The presence of a few low molecular weight VWF multimers in culture medium was in contrast to the existence only of dimers in patient's plasma. This might be explained by instability of the low molecular weight VWF multimers composed of mutant VWF monomers, and enhanced clearance of them in plasma.

Both patients with type 2A showed a smeary multimer pattern without distinguishable triplet structures indicating altered susceptibility to VWF proteolysis by ADAMTS13. Since efficiency of *in vitro* proteolysis of recombinant p.Cys2085Tyr/WT and p.Cys2327Trp/WT by rADAMTS13 was not changed compared with rVWF-WT, the altered proteolysis of mutated VWF in plasma is likely not an intrinsic property of the mutations but rather the result of strong reduction of VWF:Ag level in plasma or unequal experimental and circulation conditions.

Molecular modeling of the cysteine disulfide bonds on the C1, C5 and C6 domains (update domain designations) suggests a number of hypotheses consistent with our experimental results. Our homology models for the C

domains revealed that the cysteine residues p.Cys2283, p.Cys2619 and p.Cys2676 are involved in intra-chain/intra-domain disulfide bonds (Figure 4.7) in C1, C5 and C6, respectively, consistent with the predicted disulfide assignment suggested by Zhou *et al.* 2012.[19] The anomalous introduction of a surface charge with the p.Cys2283Arg substitution might influence interaction on the surface of the domain and the large Arg side chain might result in intra-domain instability. The –RH Staple configuration shown by the disulfide bonds involving p.Cys2619 residue is typical of disulfide bonds categorized as "allosteric" disulfide bonds responsible for regulation of protein functions depending on whether they break or form.[118,119] Therefore, this bond is critical to the overall stability of the domain since the mutation p.Cys2619Tyr in spite of breaking a disulfide bond doesn't show a remarkable change in modeled surface exposure (accessible surface area and charge) during simulation (Table 4.4; Figure 4.8, Panel C). Accommodating the large aromatic Phe side chain in the p.Cys2676Phe mutation in the C6 domain might result in intra-domain steric clashes which could damage the overall protein scaffold, and possibly cause decreased protein stability (Figure 4.8, Panel Diii). Therefore, the mutations p.Cys2283Arg, p.Cys2619Tyr and p.Cys2676Phe all may result in unstable domains. This is reflected by changes in the trajectory RMSDs, radius of gyrations (during simulation) as well as high folding energy change values for all these mutations. The total reduced expression VWF levels in our study also indicated protein instability for all these mutations which is in agreement with the *in sillico* data. Our C1 homology model and previous reports suggest that p.Cys2327 might be one of the unpaired cysteines participating in inter-domain disulfide bond with the neighbouring p.Cys2632 from the C2 domain.[19] The p.Cys2327Trp is also distinguished from the other mutants in our expression analysis by an electrophoretic mobility shift for the multimer bands confirming a major conformational change in the protein. This raises the possibility that the mutation of this cysteine to the aromatic Trp residue might create a steric interference at the point of contact for C2 domain as well as C1 domain from the opposite monomer resulting in a conformationally altered protein. Interestingly, this mutation unlike the other C-domain mutations, is not predicted to result in a large folding energy change suggesting that the variant may not affect protein stability in spite of the conformational change. This correlates with our *in vitro*

expression results where total expression level was similar to that of the wild type VWF. Interestingly, Tjernberg et al have reported mobility shift in multimer for substitutions at p.Cys2362 in the C2 domain which is most likely the disulfide-bond partner of p.Cys2327 in C1 domain .[120] Although we did not perform any structural modeling for the D4 domain, it was predicted that p.Cys2085 residue in D4 domain participate in intrachain disulfide bond.[19] The introduction of large Arg side chain will disrupt the disulfide bond, and might cause domain instability.

In summary, the current structural analysis showed that mutations eliminating these cysteine residues could induce misfolding of the respective domains. We speculate that such domain misfoldings might influence dimeric bouquet formation and consequently helical assembly of tubules and storage. Therefore, VWF secretion can be defected since tubular packing of VWF is prerequisite for physiological VWF unfurling upon exocytosis.[26, 30, 31] Moreover, recent findings stated that dimeric bouquet formation facilitates N-terminal disulphide linkage between VWF dimers which is colinear with assembly in tubules.[31, 32] Accordingly, we assume that defects in multimerization might be attributed to disruption in zipping up of misfolded C domains into dimeric bouquet structures.

In conclusion, our results indicates that the above described cysteine residues have a crucial role in accurate folding of D4 and C1, C5 and C6 domains (corresponding to original D4, B and C domains) required for proper arrangement of VWF dimer bouquets and their incorporation into growing tubules in nascent WPBs. This study demonstrates that these mutations disrupt storage, and secretion of VWF through a common pathological mechanism, although their eventual outcome on multimerization might differ because of sub-molecular differences in structural alteratnations.

References

1. Goodeve AC. The genetic basis of von Willebrand disease. Blood Rev 2010; 24: 123-34.

2. Luo GP, Ni B, Yang X, Wu YZ. Von Willebrand factor: more than a regulator of hemostasis and thrombosis. Acta Haematol 2012;128:158-69.

3. Lyons SE, Ginsburg D. Molecular and cellular biology of von Willebrand factor. Trends Cardiovasc Med 1994;4(1):34-9.

4. Hohenstein K, Griesmacher A, Weigel G, Golderer G, Ott HW. Native multimer analysis of plasma and platelet von Willebrand factor compared to denaturing separation: implication for the interpretation of satellite bands. Electrophoresis 2011;32(13):1684-91.

5. Sadler JE. von Willebrand factor: two sides of a coin. J Thromb Haemost 2005;3:1702-9.

6. Szántó T, Joutsi-Korhonen L, Deckmyn H, Lassila R. New insights into von Willebrand disease and platelet function. Semin Thromb Hemost 2012;38:55-63.

7. James PD, Goodeve AC. von Willebrand disease. Genet Med 2011;13(5):365-76.

8. Mancuso DJ, Tuley EA, Westfield LA, Worrall NK, Shelton-Inloes BB, Sorace JM, et al. Structure of the gene for human von Willebrand factor. J Biol Chem 1989; 264: 19514-27.

9. Castaman G, Federici AB, Rodeghiero F, Mannucci PM. Von Willebrand's disease in the year 2003: towards the complete identification of gene defects for correct diagnosis and treatment. Haematologica 2003; 88:94-108.

10. Keeney S, Bowen D, Cumming A, Enayat S, Goodeve A, Hill M. The molecular analysis of von Willebrand disease: a guideline from the UK Haemophilia Centre Doctors' Organisation Haemophilia Genetics Laboratory Network. Haemophilia 2008; 14: 1099-111.

11. Kasatkar P, Shetty S, Ghosh K. VWF pseudogene: Mimics, masks and spoils. Clin Chim Acta 2010;411(7-8):607-9.

12. Sadler JE. Biochemistry and genetics of von Willebrand factor. Annu Rev Biochem 1998;67:395-424.

13. Millar CM, Brown SA. Oligosaccharide structures of von Willebrand factor and their potential role in von Willebrand disease. Blood Rev 2006;20(2):83-92.

14. Lenting PJ, Casari C, Christophe OD, Denis CV. von Willebrand factor: the old, the new and the unknown. J Thromb Haemost 2012;10(12):2428-37.

15. Sadler JE. von Willebrand factor assembly and secretion. J Thromb Haemost 2009;7(Suppl. 1):24-7.

16. Schneppenheim R, Budde U. von Willebrand factor: the complex molecular genetics of a multidomain and multifunctional protein. J Thromb Haemost 2011;9 Suppl 1:209-15.

17. de Wit RT, van Mourik JA. Biosynthesis, processing and secretion of von Willebrand factor: biological implications. Best practice and research clonical haematology 2001;14(2):241-55.

18. Schneppenheim R. The pathophysiology of von Willebrand disease: therapeutic implications. Thrombosis Research 2011; 128: S3-S7.

19. Zhou YF, Eng ET, Zhu J, Lu C, Walz T, Springer TA. Sequence and structure relationships within von Willebrand factor. Blood 2012;120(2):449-58.

20. Metcalf DJ, Nightingale TD, Zenner HL, Lui-Roberts WW, Cutler DF. Formation and function of Weibel-Palade bodies. Journal of Cell Science 2008;121(1):19-27.

21. Katsumi A, Tuley EA, Bodó I, Sadler JE. Localization of disulfide bonds in the cystine knot domain of human von Willebrand factor. J Biol Chem 2000;275(33):25585-94.

22. Purvis AR, Gross J, Dang LT, Huang RH, Kapadia M, Townsend RR, et al.. Two Cys residues essential for von Willebrand factor multimer assembly in the Golgi. Proc Natl Acad Sci U S A 2007;104(40):15647-52.

23. McGrath RT, McRae E, Smith OP, O'Donnell JS. Platelet von Willebrand factor-structure, function and biological importance. British Journal of Haematology 2010;148(6):834-43.

24. Jenkins PV, O'Donnell JS. ABO blood group determines plasma von Willebrand factor levels: a biologic function after all? Transfusion 2006;46(10):1836-44.

25. O'Donnell J, Boulton FE, Manning RA, Laffan MA. Amount of H antigen expressed on circulating von Willebrand factor is modified by ABO blood group

genotype and is a major determinant of plasma von Willebrand factor antigen levels. Arterioscler Thromb Vasc Biol 2002 ;22(2):335-41.

26. Michaux G, Abbitt KB, Collinson LM, Haberichter SL, Norman KE, Cutler DF. The physiological function of von Willebrand's factor depends on its tubular storage in endothelial Weibel-Palade bodies. Dev Cell 2006;10(2):223-32.

27. Valentijn KM, Sadler JE, Valentijn JA, Voorberg J, Eikenboom J. Functional architecture of Weibel-Palade bodies. Blood 2012;117(19):5033-43.

28. Blombäck M, Eikenboom J, Lane D, Denis C, Lillicrap D. Von Willebrand disease biology. Haemophilia 2012;18 Suppl 4:141-7.

29. Hannah MJ, Williams R, Kaur J, Hewlett LJ, Cutler DF. Biogenesis of Weibel-Palade bodies. Seminars in Cell & Development Biology 2002;13: 313-24.

30. Huang RH, Wang Y, Roth R,Yu X, Purvis AR, Heuser JE, et al. Assembly of Weibel-Palade body-like tubules from N-terminal domains of von Willebrand factor. Proc Natl Acad Sci U S A 2008;105(2):482-7.

31. Zhou YF, Eng ET, Nishida N, Lu C, Walz T, Springer TA. A pH-regulated dimeric bouquet in the structure of von Willebrand factor. EMBO J 2011;30(19):4098-111.

32. Springer TA. Biology and physics of von Willebrand factor concatamers. J Thromb Haemost 2011;9 Suppl 1:130-43.

33. van Mourik JA, de Wit TR, Voorberg J. Biogenesis and exocytosis of Weibel-Palade bodies. Histochem Cell Biol 2002;117:113-22.

34. De Ceunynck K, De Meyer SF, Vanhoorelbeke K. Unwinding the von Willebrand factor strings puzzle Blood. 2013;121(2):270-7.

35. Ganderton T, Wong JW, Schroeder C, Hogg PJ. Lateral self-association of VWF involves the Cys2431-Cys2453 disulfide/dithiol in the C2 domain. Blood 2011;118(19):5312-8.

36. Hassenpflug WA, Budde U, Obser T, Angerhaus D, Drewke E, Schneppenheim S, et al. Impact of mutations in the von Willebrand factor A2 domain on ADAMTS13-dependent proteolysis. Blood 2006;107(6):2339-45.

37. Starke RD, Ferraro F, Paschalaki KE, Dryden NH, McKinnon TA, Sutton RE, et al. Endothelial von Willebrand factor regulates angiogenesis. Blood 2011;117(3):1071-80.

38. Tjernberg AP. 2007. The effect of mutated cysteine residues in von Willebrand factor. Ph.D. thesis, Leiden University, Netherlands.192pp.

39. Terraube V, O'Donnell JS, Jenkins PV. Factor VIII and von Willebrand factor interaction: biological, clinical and therapeutic importance. Haemophilia 2010;16(1):3-13.

40. James PD, Lillicrap D, Mannucci PM. Alloantibodies in von Willebrand Disease. Blood 2013 Jan [Epub ahead of print].

41. Federici AB, Canciani MT. Clinical and laboratory versus molecular markers for a correct classification of von Willebrand disease. Haematologica 2009;94(5):610-5.

42. Sadler JE, Budde U, Eikenboom JC, Favaloro EJ, Hill FG, Holmberg L, et al. Update on the pathophysiology and classification of von Willebrand disease: a report of the Subcommittee on von Willebrand Factor. J Thromb Haemost 2006; 4: 2103-14.

43. Budde U. Diagnosis of von Willebrand disease subtypes: implications for treatment. Haemophilia 2008; 14: 27-38.

44. Castaman G, Montgomery RR, Meschengieser SS, Haberichter SL, Woods AI, Lazzari MA. Von Willebrand's disease diagnosis and laboratory issues. Haemophilia 2010;16(Supple. 5):67-73.

45. Budde U, Pieconka A, Will K, Schneppenheim R. Laboratory testing for von Willebrand disease: contribution of multimer analysis to diagnosis and classification. Semin Thromb Hemost 2006;32:514-21.

46. Fischer BE, Thomas KB, Schlokat U, Dorner F. Triplet structure of human von Willebrand factor. Biochem J 1998;331:483-8.

47. Starke RD, Paschalaki KE, Dyer CE, Harrison-Lavoie KJ, Cutler JA, McKinnon TA, et al. Cellular and molecular basis of von Willebrand disease: studies on blood outgrowth endothelial cells. Blood. 2013 Jan [Epub ahead of print].

48. Franchini M, Capra F, Targher G, Montagnana M, Lippi G. Relationship between ABO blood group and von Willebrand factor levels: from biology to clinical implications.Thromb J 2007; 5: 14.

49. Sadler JE. Low von Willebrand factor: sometimes a risk factor and sometimes a disease. Hematology Am Soc Hematol Educ Program 2009:106-12.

50. van Schooten CJ, Tjernberg P, Westein E, Terraube V, Castaman G, Mourik JA, et al. Cysteine-mutations in von Willebrand factor associated with increased clearance. J Thromb Haemost 2005;3(10):2228-37.

51. Lillicrap D. Genotype/phenotype association in von Willebrand disease: is the glass half full or empty? J Thromb Haemost 2009; 7: 65-70.

52. Lillicrap D. Von Willebrand disease - phenotype versus genotype: deficiency versus disease. Thromb Res 2007; 120 Suppl 1: S11-6.

53. Federici AB. Classification of inherited von Willebrand disease and implications in clinical practice. Thrombosis Research 2009; 124: S2-S6.

54. Xu AJ, Springer TA. Mechanisms By Which von Willebrand Disease Mutations Destabilize the A2 Domain. J Biol Chem. 2013 Jan [Epub ahead of print]

55. James PD, Lillicrap D. von Willebrand disease: Clinical and laboratory lessons learned from the large von Willebrand disease studies. Am. J. Hematol 2012; 87:S4-S11.

56. Castaman G, Lethagen S, Federici AB, Tosetto A, Goodeve A, Budde U, et al. Response to desmopressin is influenced by the genotype and phenotype in type 1 von Willebrand disease (VWD): results from the European Study MCMDM-1VWD. Blood 2008;111(7):3531-9.

57. Tuohy E, Litt E, Alikhan R. Treatment of patients with von Willebrand disease. Journal of blood medicine 2011;2:49-57.

58. Peake I, Goodeve A. Type 1 von Willebrand disease. Journal of Thrombosis and Haemostasis 2007; 5: 7–11.

59. Schneppenheim R, Budde U, Obser T, Brassard J, Mainusch K, Ruggeri ZM et al. Expression and characterization of von Willebrand factor dimerization defects in different types of von Willebrand disease. Blood 2001; 97: 2059-66.

60. Schneppenheim R, Lenk H, Obser T, Oldenburg J, Oyen F, Schneppenheim S, et al. Recombinant expression of mutations causing von Willebrand disease type Normandy: characterization of a combined defect of factor VIII binding and multimerization. Thromb Haemost 2004;92(1):36-41.

61. Collins PW, Cumming AM, Goodive AC, et al. Type 1 von willebrand disease: application of emerging data to clinical practice. Haemophilia 2008; 14: 685-696.

62. Goodive A, Eikenboom J, Castaman G, Lillicrap D. Phenotype and genotype of a cohort of families historically diagnosed with type 1 von Willebrand disease in the European study, Molecular and Clinical Markers for the Diagnosis and Management of Type 1 von Willebrand Disease (MCMDM-1VWD). Blood 2007; 109:112-21.

63. James PD, Notley C, Hegadorn C, Leggo J, Tuttle A, Tinlin S, et al. The mutational spectrum of type 1 von Willebrand disease: results from a Canadian cohort study. Blood 2007; 109: 145-54.

64. Cumming A, Grundy P, Keeney S, Lester W, Enayat S, Guilliatt A ,et al. An investigation of the von Willebrand factor genotype in UK patients diagnosed to have type 1 von Willebrand disease. Thromb Haemost 2006; 96: 630-41.

65. Budde U, Schneppenheim R, Eikenboom J, Goodeve A, Will K, Drewke E, Castaman G et al. Detailed von Willebrand factor multimer analysis in patients with von Willebrand disease in the European study, molecular and clinical markers for the diagnosis and management of type 1 von Willebrand disease (MCMDM-1VWD). J Thromb Haemost 2008; 6:762-71.

66. Miller SA, Dykes DD, Polesky HF. A simple salting out procedure for extracting DNA from human nucleated cells. Nucleic Acids Res 1988; 16: 1215.

67. Ng PC, Henikoff S. SIFT: Predicting amino acid changes that affect protein function. Nucleic Acids Res 2003; 31: 3812-4.

68. Yadegari H, Driesen J, Hass M, Budde U, Pavlova A, Oldenburg J. Large deletions identified in patients with von Willebrand disease using multiple ligation-dependent probe amplification. J Thromb Haemost 2011; 9:1083-6.

69. Huizinga EG, Tsuji S, Romijn RA, Schiphorst ME, de Groot PG, Sixma JJ, et al. Structures of glycoprotein Ib alpha and its complex with von Willebrand factor A1 domain. Science 2002; 297:1176-9.

70. Emsley J, Cruz M, Handin R, Liddington R. Crystal structure of the von Willebrand Factor A1 domain and implications for the binding of platelet glycoprotein Ib. J Biol Chem 1998; 273:10396-401.

71. Pettersen EF, Goddard TD, Huang CC, Couch GS, Greenblatt DM, Meng EC, et al. UCSF Chimera-visualization system for exploratory research and analysis. J Comput Chem 2004; 25:1605-12. http://www.cgl.ucsf.edu/chimera/ , Accessed November 6, 2006.

72. Mills J.E.J, Dean P.M. Three-dimensional hydrogen-bond geometry and probability information from a crystal survey *J Comput-Aided Mol Des* 1996; 10: 607.

73. James PD, Paterson AD, Notley C, Cameron C, Hegadorn C, Tinlin S, et al. Genetic linkage and association analysis in type 1 von Willebrand disease: results from the Canadian Type 1 VWD Study. J Thromb Haemost 2006; 4: 783–92.

74. Eikenboom J, Van Marion V, Putter H, Goodeve A, Rodeghiero F, Castaman G, et al. Linkage analysis in families diagnosed with type 1 von Willebrand disease in the European study, molecular and clinical markers for the diagnosis and management of type 1 VWD. J Thromb Haemost 2006; 4: 774–82.

75. Hermans C, Batlle J. Autosomal dominant von Willebrand disease type 2M. Acta Haematol 2009; 121: 139-44.

76. Corrales I, Catarino S, Ayats J, Arteta D, Altisent C, Parra R, et al. High-throughput molecular diagnosis of von Willebrand disease by next generation sequencing methods. Haematologica 2012; 97 [Epub ahead of print].

77. Robertson JD, Yenson PR, Rand ML, Blanchette VS, Carcao MD, Notley C, et al. Expanded phenotype correlations in a pediatric population with type 1 von Willebrand disease. J Thromb Haemost 2011; 9: 1752-60.

78. Sutherland MS, keeney S, Bolton-Maggs PHB, Hay CR, Will A, Cumming AM. The mutation spectrum associated with type 3 von Willebrand disease in a cohort of patients from the North West of England. Haemophilia 2009; 15: 1048-57.

79. Baronciani L, Cozzi G, Canciani MT, Peyvandi F, Srivastava A, Federici AB, et. al. Molecular defects in type 3 von Willebrand disease: updated results from 40 multiethnic patients. Blood Cells, Molecules, and Diseases 2003; 30: 264-70.

80. Baronciani L, Cozzi G, Canciani MT, Peyvandi F, Srivastava A, Federici AB, et. al. Molecular characterization of a multiethnic group of 21 patients with type 3 von Willebrand disease. Thromb Haemost 2000; 84: 536-40.

81. Gadisseur A, van der Planken M, Schroyens W, Berneman Z, Michiels JJ. Dominant von Willebrand disease type 2M and 2U are variable expressions of

one distinct disease entity caused by loss-of-function mutations in the A1 domain of the von Willebrand factor gene. Acta Haematol 2009; 121:145-53.

82. Corrales I, Ramirez L, Altisent C, Parra R, Vidal F. Rapid molecular diagnosis of von Willebrand disease by direct sequencing. Detection of 12 novel putative mutations in *VWF* gene. Thromb Haemost 2009; 101: 570-6.

83. James PD, Notley C, Hegadorn C, Poon MC, Walker I, Rapson D et al. Challenges in defining type 2M von Willebrand disease: results from a Canadian cohort study. J Thromb haemost 2007; 5: 1914-22.

84. Berber E, James PD, Hough C, Lillicrap D. An assessment of the pathologenic significance of the R924Q von Willebrand factor substitution. J Thromb Haemost 2009; 7: 1672-9.

85. Hickson N, Hampshire D, Winship P, Goudemand J, Schneppenheim R, Budde U, et al, on behalf of the MCMDM-1VWD and ZPMCB-VWD Study Groups. von Willebrand factor variant p.Arg924Gln marks an allele associated with reduced von Willebrand factor and factor VIII levels. J Thromb Haemost 2010; 8: 1986–93.

86. Eikenboom J, Hilbert L, Ribba AS, Hommais A, Habart D, Messenger S, et al. Expression of 14 von Willebrand factor mutations identified in patients with type 1 von Willebrand disease from the MCMDM-1VWD study. J Thromb Haemost 2009; 7:1304-12.

87. Allen S, Abuzenadah AM, Blagg JL, Hinks J, Nesbitt IM, Goodeve AC, et al. Two novel type 2N von Willebrand disease-causing mutations that result in defective factor VIII binding, multimerization, and secretion of von Willebrand factor. Blood 2000; 95: 2000-7.

88. McKinnon TA, Goode EC, Birdsey GM, Nowak AA, Chan AC, Lane DA, et al. Specific N-linked glycosylation sites modulate synthesis and secretion of von Willebrand factor. Blood 2010;116: 640-8.

89. Corrales I, Ramirez L, Altisent C, Parra R, Vidal F. The study of the effect of splicing mutations in von Willebrand factor using RNA isolated from patients' platelets and leukocytes. J Thromb Haemost 2011; 9: 679-88.

90. Zhang Q, Zhou YF, Zhang CZ, Zhang X, Lu C, Springer TA. Structural specializations of A2, a force-sensing domain in the ultralarge vascular protein von Willebrand factor. Proc Natl Acad Sci U S A 2009;106: 9226-31.

91. Schneppenheim R, Castaman G, Federici AB, Kreuz W, Marschalek R, Oldenburg J et al. A common 253-kb deletion involving VWF and TMEM16B in German and Italian patients with severe von Willebrand disease type 3. J Thromb Haemost. 2007; 5: 722-8.

92. Sutherland MS, Cumming AM, Bowman M, Bolton-Maggs PHB, Bowen DJ, Collins PW et al. A novel deletion mutation is recurrent in von Willebrand disease types 1 and 3. Blood. 2009; 114 (5): 1091-8.

93. Xie F, Wang X, Cooper DN, Chuzhanova N, Fang Y, Cai X, et al. A novel Alu-mediated 61-kb deletion of the von Willebrand factor (*VWF*) gene whose breakpoints co-locate with putative matrix attachment regions. Blood Cells, Molecules, and Diseases 2006;36: 385-91.

94. Mohl A, Marschalek R, Masszi T, Nagy E, Obser T, Oyen F, et al. An Alu-mediated novel large deletion is the most frequent cause of type 3 von Willebrand disease in Hungary. J Thromb Haemost 2008;6:1729-35.

95. Goodeve AC. When 1 plus 1 equals 3 in VWD. Blood 2009;114(5):933-4.

96. Jacquemin M, Lavend'homme R, Benhida A, Vanzieleghem B, d'Oiron R, Lavergne JM, et al. A novel cause of mild/moderate hemophilia A: mutations scattered in the factor VIII C1 domain reduce factor VIII binding to von Willebrand factor. Blood 2000;96(3):958-65.

97. Bernardi F, Patracchini P, Gemmati D, Pinotti M, Schwienbacher C, Ballerini G, et al. In-frame deletion of von Willebrand factor A domains in a dominant type of von Willebrand disease. Hum Mol Genet 1993; 2: 545-8.

98. Casari C, Pinotti M, Lancellotti S, Adinolfi E, Casonato A, Cristofaro RD, et al. The dominant-negative von Willebrand factor gene deletion p.P1127_C1948delinsR: molecular mechanism and modulation. Blood 2010; 116(24): 5371-6.

99. Eikenboom J, Van Marion V, Putter H, Goodeve A, Rodeghiero F, Castaman G, et al. Linkage analysis in families diagnosed with type 1 von Willebrand disease in the European study, molecular and clinical markers for the diagnosis and management of type 1 VWD. J Thromb Haemost 2006; 4(4):774-82.

100. Haberichter SL, Fahs SA, Montgomery RR. von Willebrand factor storage and multimerization: 2 independent intracellular processes. Blood 2000;96(5):1808-15.

101. Jacobi PM, Gill JC, Flood VH, Jakab DA, Friedman KD, Haberichter SL. Intersection of mechanisms of type 2A VWD through defects in VWF multimerization, secretion, ADAMTS-13 susceptibility, and regulated storage. Blood 2012;119(19):4543-53.

102. Hilbert L, Federici AB, Baronciani L, Dallagiovanna S, Mazurier C. A new candidate mutation, G1629R, in a patient with type 2A von Willebrand's disease: basic mechanisms and clinical implications. Haematologica 2004;89(9):1128-33.

103. Yadegari H, Driesen J, Pavlova A, Biswas A, Hertfelder HJ, Oldenburg J. Mutation distribution in the von Willebrand factor gene related to the different von Willebrand disease (VWD) types in a cohort of VWD patients. Thromb Haemost 2012;108(4):662-71.

104. Bowman M, Mundell G, Grabell J, Hopman WM, Rapson D, Lillicrap D et al. Generation and validation of the Condensed MCMDM-1VWD Bleeding Questionnaire for von Willebrand disease. J Thromb Haemost 2008;6(12):2062-6.

105. Schneppenheim R, Michiels JJ, Obser T, Oyen F, Pieconka A, Schneppenheim S, et al. A cluster of mutations in the D3 domain of von Willebrand factor correlates with a distinct subgroup of von Willebrand disease: type 2A/IIE. Blood 2010;115(23):4894-901.

106. Wang JW, Valentijn KM, de Boer HC, Dirven RJ, van Zonneveld AJ, Koster AJ, et al. Intracellular storage and regulated secretion of von Willebrand factor in quantitative von Willebrand disease. J Biol Chem. 2011;286(27):24180-8.

107. Wu S, Zhang Y. LOMETS: a local meta-threading-server for protein structure prediction. Nucleic Acids Res. 2007;35(10):3375-3382.

108. Krieger E, Koraimann G, Vriend G. Increasing the precision of comparative models with YASARA NOVA--a self-parameterizing force field. Proteins 2002;47(3):393-402.

109. Davis IW, Leaver-Fay A, Chen VB, Block JN, Kapral GJ, Wang X, et al. MolProbity: all-atom contacts and structure validation for proteins and nucleic acids. Nucleic Acids Res 2007;35:W375-83.

110. Comeau SR, Gatchell DW, Vajda S, Camacho CJ. ClusPro: an automated docking and discrimination method for the prediction of protein complexes. Bioinformatics 2004;20(1):45-50.

111. Van Durme J, Delgado J, Stricher F, Serrano L, Schymkowitz J, Rousseau F. A graphical interface for the FoldX forcefield. Bioinformatics 2011;27(12):1711-2.

112. Krieger E, Joo K, Lee J, Lee J, Raman S, Thompson J, et al. Improving physical realism, stereochemistry, and side-chain accuracy in homology modeling: Four approaches that performed well in CASP8. Proteins. 2009;77 Suppl 9:114-22.

113. Castaman G, Giacomelli SH, Jacobi P, Obser T, Budde U, Rodeghiero F, et al. Homozygous type 2N R854W von Willebrand factor is poorly secreted and causes a severe von Willebrand disease phenotype. J Thromb Haemost 2010;8:2011-6.

114. Wang JW, Groeneveld DJ, Cosemans G, Dirven RJ, Valentijn KM, Voorberg J et al. Biogenesis of Weibel-Palade bodies in von Willebrand's disease variants with impaired von Willebrand factor intrachain or interchain disulfide bond formation. Haematologica 2012 ;97(6):859-66.

115. Castaman G, Giacomelli SH, Jacobi PM, Obser T, Budde U, Rodeghiero F, et al. Reduced von Willebrand factor secretion is associated with loss of Weibel-Palade body formation. J Thromb Haemost 2012;10:951-8.

116. Haberichter SL, Budde U, Obser T, Schneppenheim S, Wermes C, Schneppenheim R. The mutation N528S in the von Willebrand factor (VWF) propeptide causes defective multimerization and storage of VWF. Blood 2010;115(22):4580-7.

117. Michaux G, Hewlett LJ, Messenger SL, Goodeve AC, Peake IR, Daly ME, et al. Analysis of intracellular storage and regulated secretion of 3 von Willebrand disease-causing variants of von Willebrand factor. Blood 2003;102(7):2452-8.

118. Schmidt B, Ho L, Hogg PJ. Allosteric disulfide bonds. Biochemistry 2006;45(24):7429-33.

119. Chen VM, Hogg PJ. Allosteric disulfide bonds in thrombosis and thrombolysis. J Thromb Haemost 2006;4(12):2533-41.

120. Tjernberg P, Castaman G, Vos HL, Bertina RM, Eikenboom JC. Homozygous C2362F von Willebrand factor induces intracellular retention of mutant von Willebrand factor resulting in autosomal recessive severe von Willebrand disease. Br J Haematol 2006;133(4):409-18.

List of publications

- Yadegari H, Driesen J, Pavlova A, Biswas A, Ivaskevicius V, Klamroth R, Oldenburg J. Insights into pathological mechanisms of missense mutations in C-terminal domains ff von Willebrand factor causing qualitative or quantitative von Willebrand disease. Haematologica 2013 [In Press]. Impact factor of journal: 6.4.

- Yadegari H, Driesen J, Pavlova A, Biswas A, Hertfelder HJ, Oldenburg J. Mutation distribution in the von Willebrand factor gene related to the different von Willebrand disease (VWD) types in a cohort of VWD patients. Thromb Haemost. 2012;108(4):662-671. Impact factor of journal: 5.04.

- Yadegari H, Driesen J, Hass M, Budde U, Pavlova A, Oldenburg J. Large deletions identified in patients with von Willebrand disease using multiple ligation-dependent probe amplification. J Thromb Haemost. 2011;9:1083-1086. Impact factor of journal: 5.7.

- Sabouri A, Fazilati M, **Yadegari H**. Comparison the effectiveness of extraction protocols phenol-chloroform-silica and guanidinium thiocyanate-silica in recovering DNA from human skeletal remains. Scientific Journal of Forensic Medicine of Iran, 2008; 14(51):159-165.

- Sabouri A, **Yadegari H.** Estimation of efficiency of blood group in comparison with DNA Typing tests in disputed paternity. Scientific Journal of Forensic Medicine of Iran, 2007; 13(1):25-29.

- Sabouri A, Ghodousi A, **Yadegari H**, Moshksar E . Extraction and evaluation of DNA from tooth using modified Guanidinium Thiocyanate_Silica method in unknown cadaver referred to the legal medicine center of Esfahan. Scientific Journal of Forensic Medicine of Iran, 2005;11(2):71-76.

Oral and poster presentations

Oral presentations:

- Yadegari H, Driesen J, Pavlova A, Biswas A, Ivaskevicius V, Klamroth R, Oldenburg J. Functional characterization of five von Willebrand factor missense mutations affecting cysteine residues. 57th Annual Meeting of the Gesellschaft für Thrombose- und Hämostaseforschung (GTH): Munich, Germany, February 20 -23. 2013.

- Yadegari H, Driesen J, Pavlova A, Biswas A, Hertfelder HJ, Oldenburg J. Von Willebrand disease: genotype-phenotype correlation. 44. Jahreskongress der Deutschen Gesellschaft für Transfusionsmedizin und Immunhämatologie (DGTI): Hannover. Germany, 27 – 30 September 2011.

- Alireza Sabouri, Arash Ghodousi, **Hamideh Yadegari**, Elham Moshksar. Extraction and evaluation of DNA from tooth using modified Guanidinium Thiocyanate_Silica method in unknown cadaver referred to the legal medicine center of Esfahan. 17th meeting of the international association forensic sciences: Hong Kong, China, 21-26 August 2005.

Poster:

- Yadegari H., Driesen J., Pavlova A., Oldenburg J. Expression Studies of von Willebrand Factor Missense Mutations Causing Type 1 or Type 2 VWD. International Congress of the World Federation of Hemophilia: Paris, France, 8-12 Juli 2012.

- Yadegari H., Driesen J., Pavlova A., Dermer H., Schüring I., Vidovic N. Hertfelder H.-J., Oldenburg J. Genotype-Phenotype Correlation in Von Willebrand Disease. Congress of the International Society on Thrombosis and Haemostasis: Kyoto, Japan, 23-28 July 2011.

- Yadegary H, Y Shafeghati, H Najmabadi, M Ohadi. Combined analysis of the factor VIII gene intragenic markers for carrier detection and prenatal diagnosis of haemophilia A in Iran. International Genetic Congress,United Arab Emirate, 9-11 December 2003.

- Yadegari H. Preimplantation Genetic Diagnosis. The First Students Congress of Biology and Biotechnology, Esfahan, Iran 2001.

Acknowledgements

First of all I would like to express my sincerest gratitude to my supervisor Prof. Dr Johannes Oldenburg for giving me the opportunity to perform my PhD thesis in institute of Experimental Haematology and Transfusion Medicine. His ability to transfer enthusiasm and knowledge has provided the basis for me to accomplish this work.

Moreover, I am grateful to Dr. Julia Driesen for her guidance and support in preparing this thesis.

I sincerely thank PD Dr. med Anni Pavlova for scientific advices, teaching me her valuable experiences and her support in accompanying my thesis.

I am grateful to Dr. Arijit Biswas for his support for doing *in Silico* structural analysis and his assistance during my work.

I wish to thank Ms Helena Dermer and Ms Inga Schüring for their excellent technical assistance. I am also thankful to Prof. Dr. med. B. Pötzsch and his lab technicians for help in measuring the antigen levels and activity levels of my samples in their laboratory.

Sincere thanks to Dr. Zaid Aburubaiha and Priv. Doz. Dr. Rainer Schwaab for their help in cell culture lab over the last years.

I also thank all my colleagues in institute of Experimental Haematology and Transfusion Medicine of University clinic Bonn for their support, understanding and making a friendly working environment.

Last but not least I wish to express my deepest gratitude to my family, my parents and my siblings who have supported and encouraged me entire my life with care, love and good advice.